

Unravelling the influence of water depth and wave energy on the facies diversity of shelf carbonates

SAM J. PURKIS, GWILYM P. ROWLANDS and JEREMY M. KERR

National Coral Reef Institute, Nova Southeastern University Oceanographic Center, 8000 N. Ocean Drive, Dania Beach, FL 33004, USA (E-mail: purkis@nova.edu)

Associate Editor – John Reijmer

ABSTRACT

Carbonate sequence stratigraphy is founded on the principle that changes in relative sea-level are recorded in the rock record by the accumulation of sediment with relative water depth-dependent attributes. While at the scale of a shelf to basin transect, facies clearly arrange by water depth, the relation blurs for depths <40 m, the most vigorous zone of carbonate production. The reason for this change in behaviour is two-fold. Firstly, in shallow water, the intrinsic processes of storm and wave reworking influence the seabed through submarine erosion and sediment redistribution. Secondly, facies diversity tends to be greater in shallow water than deep water because of a greater diversity in grain producers. Remote sensing imagery, field observations and hydrodynamic models for two reef-rimmed shore-attached carbonate platforms in the Red Sea show neither water depth nor energy regime to be reliable indicators of facies type when considered in isolation. Considered together, however, the predictive power of the two variables rises significantly. The results demonstrate it to be an oversimplification to assume a direct link between palaeo-water depth and depositional diversity of subtidal lithofacies, while highlighting the importance of hydrodynamics in directing the accumulation of carbonate sediments in the shallow photic zone. While the size distributions of facies extents in the two focus areas follow power laws, no direct relation between the lateral continuity of the facies belts and water depth or wave height is reported. The work is relevant for the interpretation of metre-scale subtidal carbonate cycles throughout the geological record by demonstrating how caution must be applied when inferring palaeo-water depths from depositional facies.

Keywords Depositional facies, entropy, GIS, Red Sea, water depth, wave regime.

INTRODUCTION

It is a long-held tenet in carbonate geology that changes in water depth, and hence sea-level, can be recognized through analysis of the sedimentary record. Sequence stratigraphy provides the framework for understanding how sedimentary systems evolve through geological time. One method of reading the sedimentary record is through examination of lithofacies; rocks characterized by their sedimentary attributes,

such as grain size and sorting, fossil fauna and bedding structure. Examination of modern carbonate systems (in particular the Bahamas, eastern Arabian Gulf and Western Australia) has provided a broad context for the definition of 'environments of deposition' that can be applied to the rock record in order to associate sequences of lithofacies to palaeo-water depths (Ginsburg, 1956, 1975; Fischer, 1964; Laporte, 1967; Shinn *et al.*, 1969; Logan *et al.*, 1970; Liebau, 1984; Immenhauser, 2009). In the so-called

'T-Factory', because their production is tied to light and wave energy, carbonate sediments are most effectively produced in shallow water and it is in this environment of deposition that they predominantly amass (Schlager, 2003). Potential rates of accumulation are typically much greater than the rate of subsidence of the shelf or platform upon which they are deposited and, for this reason, carbonate accumulations repeatedly build up to sea-level and above. Characteristic stacks of peritidal carbonate beds, termed to be 'shallowing-upward', result. In the shallow-water sedimentary rock record, occurrences of repetitive shallowing-upward patterns of lithofacies recurrence are typically assumed to be 'allocyclic', that is they are driven by orbital forcing on eustatic sea-level (Fischer, 1964; Goodwin & Anderson, 1985; Grotzinger, 1986; Goldhammer *et al.*, 1987; Strasser, 1988; Eriksson & Simpson, 1990; Hinnov & Goldhammer, 1991; Osleger, 1991; Strasser *et al.*, 1999; Schwarzacher, 2000; Meyers, 2008; Eberli, 2013), although the pattern can also be biogenic in origin over limited scales (Wanless, 1981; Purkis & Riegl, 2005), or result from autocyclic sediment transport as theorized by Ginsburg (1971).

Autocyclic formation of peritidal carbonate cycles is proposed to arise from the repeated seaward progradation of shorelines and islands across a platform top, driven by the imbalance in size between the large open marine sources of sediment production and smaller nearshore traps. As the shoreline progrades seaward, the size of the open marine source area decreases. Eventually, reduced production of sediment no longer exceeds slow continuous subsidence and a new transgression begins (Ginsburg, 1971). Even in the absence of relative sea-level oscillations, the autocyclic model advocates processes within a sedimentary system that develops cyclic feedback loops linking sediment production, transportation and deposition and under such auspices, shoreline progradation might be a cycle-producing mechanism. While Pratt & James (1986) and Satterley (1996) provided outcrop data supporting autocyclicality, as does Strasser (1988), albeit at a limited scale, and the output of numeric forward models also backs the plausibility of autocyclicality (Burgess, 2001, 2006; Burgess *et al.*, 2001; Burgess & Wright, 2003), platform-scale evidence of the concept is scarce in the rock record and it remains challenging to tease apart cyclicality generated by factors internal to the sedimentary system versus those related to sea-level oscillation

(Schwarzacher, 2000; Peterhänsel & Egenhoff, 2008; Eberli, 2013).

Depositional topography and irregularly filled accommodation both enhance the complexity of the lateral arrangement of coevally deposited platform-top facies, as is evident in the satellite imagery for the two focus areas considered in this study. If variable bathymetry persists through time, as is typical, the lateral facies complexity that exists along single timelines permeates into cycles that display complex lateral variability in thickness and frequency, even when forced by the deterministic pendulum of orbitally driven sea-level fluctuations. Here, depositional topography prevents every climate cycle from being recognized in the sedimentary record since all sea-level fluctuations do not necessarily reach the platform top; so-called 'missed beats' (Schwarzacher, 2000; Eberli, 2013). For instance, variable numbers of cycles will be deposited across the platform top in cases where some sea-level highstands are sufficient in magnitude to flood the entire system, but others only flood topographic lows. Furthermore, sea-level cycles may not be recorded locally if thresholds were too low to create diagnostic facies changes.

James (1984) deemed the ideal shallowing-upward peritidal carbonate sequence to comprise four units: "the basinal unit which is generally thin, records the initial transgression over pre-existing deposits and so is commonly a high-energy deposit. The bulk of the sequence which may be of diverse lithologies consists of normal marine carbonate. The upper part of the sequence consists of two units: the intertidal unit within the normal range of tides; the other a supratidal unit, deposited in the area covered only by abnormal, windblown or storm tides". Each of these idealized units would be identified in the fossil record by the occurrence of lithofacies, with relative water depth-dependent attributes, stacked vertically in a non-random order. If bounded by flooding surfaces, the stack could be termed a 'parasequence' and it would be assumed that the lithofacies were deposited in lateral continuity to one another such that Walther's Law holds true (for example, Fig. 1A); a property that can be harnessed for three-dimensional reconstruction of carbonate rock bodies (Purkis & Vlaswinkel, 2012; Purkis *et al.*, 2012b). The present study was designed to ascertain whether idealized metre-scale peritidal and subtidal sequences are encountered in two Red Sea focus areas and, if they are, whether the

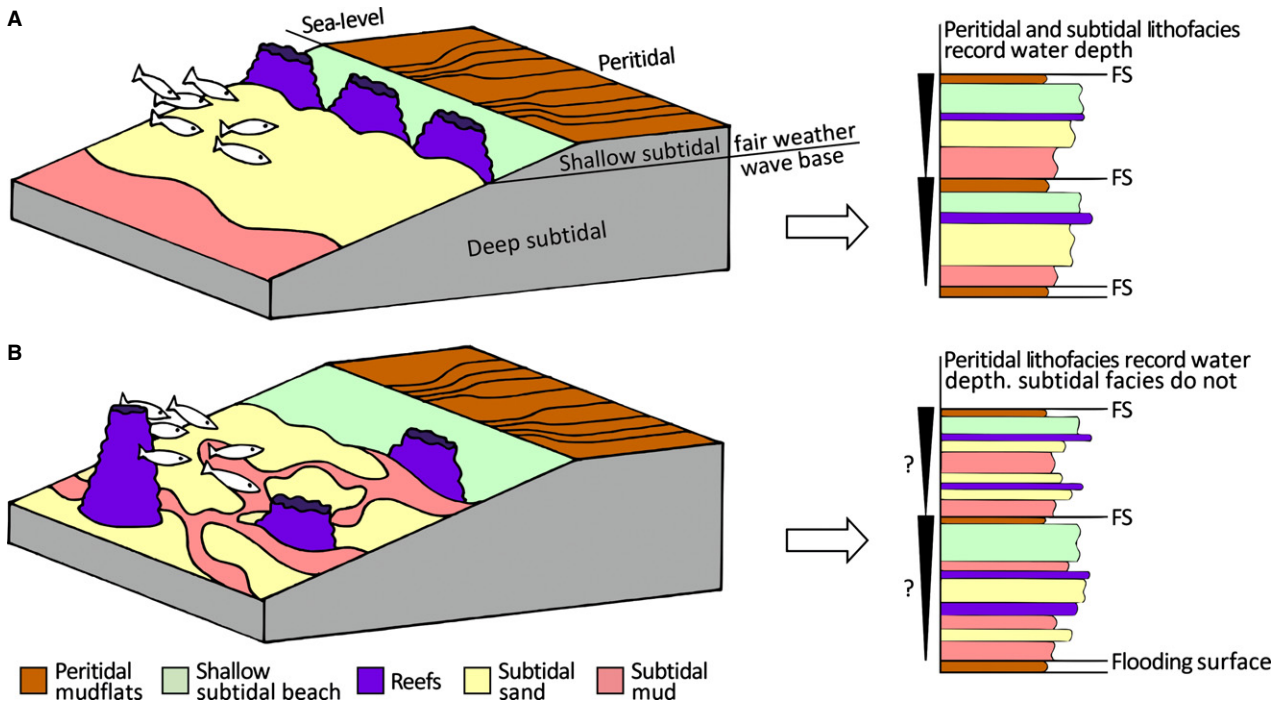


Fig. 1. Two conceptual models depicting facies accumulation in the shallow photic zone. The models show how laterally continuous shore-parallel ‘belts’ are promoted when facies are differentiated by water depth. (A) As shown in the simplified log, lateral migration of these facies belts should, when Walther’s Law applies, generate the kinds of idealized successions of carbonate strata as depicted, for example, by James (1984). Meanwhile, the consequence of facies substitutability with depth generates sedimentological heterogeneity and delivers a complex facies ‘mosaic’. (B) In this case, lateral migration of the deep subtidal facies does not deliver a log from which fluctuations in sea-level can be derived. Note that, in both scenarios, the shallow subtidal beach facies and peritidal mudflats are laterally continuous because their deposition is governed by the distinct hydrodynamics that govern this zero-depth zone. It is for this reason, along with their limited diversity that peritidal and shallow subtidal carbonate lithofacies reliably record sea-level position. Results from this study will evidence scenario (B) to be more realistic than (A) and caution on the over-interpretation of deep subtidal lithofacies to infer sea-level position in the geological record.

sequences are truly indicative of shallowing-upward cycles.

As noted by Rankey (2004), at a scale of shelf to basin transects, grain-size trends are clearly related to water depth (bathymetry). Ginsburg (1956) questioned in Florida Bay, however, the degree to which grain-size to depth relations hold in the zone of most vigorous carbonate production, which lies between the intertidal and 40 m water depth. Here, in the shallow photic zone, it is reasonable to assume that depositional control on facies occurs both from changes in relative sea-level, an allogenic process, as well as autogenic processes such as the natural redistribution of energy and sediment that cause the lateral migration of facies, creating a complex mosaic. Such uncertainties pose question marks over the degree to which systematic fining and coarsening patterns of carbonate facies in the rock record can be interpreted to represent high-

frequency metre-scale eustatic sea-level fluctuations. Note that this article uses ‘allogenic’ and ‘autogenic’ as synonyms to ‘autocyclic’ and ‘allocyclic’. The use of the term ‘genic’ versus ‘cyclic’ is varied across the literature, although the message is the same.

Wright & Burgess (2005) summarize how the understanding of where and how carbonate sediments are produced and accumulate has evolved from the rather unsophisticated concept of direct productivity-depth relations (i.e. Fig. 1A), to an appreciation that carbonate depositional environments host a continuum of different types of productive sites over wide water depth ranges, each perhaps influenced to some degree by depth, but also by a complex suite of autogenic factors (i.e. Fig. 1B). This situation leads to a facies mosaic consisting of elements that do not neatly stratify by water depth, but instead migrate and succeed one another on short scales

as a consequence of subtle environmental changes that occur much more rapidly than the generation of accommodation (Diedrich & Wilkinson, 1999; Wright & Burgess, 2005). Hence, any point atop a carbonate platform is likely to hold facies from different environments super-imposed and mixed, so-called 'palimpsest' sediments.

Through a study of the Holocene tidal flats surrounding north-west Andros Island, Maloof & Grotzinger (2012) considered the control exerted by post-glacial sea-level rise on the accumulation of peritidal carbonates versus the influence of migrating and avulsing tidal channels. Sea-level oscillation, an allogenic process, was found to dominate the autogenic (channel migration). While the work of Maloof & Grotzinger (2012) is informative, it only covers a small geographic area (10 km²); and, as reviewed and modelled by Burgess (2006), alternative scenarios probably exist where autogenic processes are as, or more, important than allogenic processes. In these situations, the use of lithofacies to identify shallowing-upward sequences becomes problematic at best, impossible at worst, and the application of sequence stratigraphic concepts for carbonates in the shallow photic zone may be less reliable than assumed. By expanding the search below the intertidal into the open marine zone of maximum carbonate production, this paper will simultaneously investigate the importance of an allogenic (water depth) and autogenic process (wave height) on the metre-scale distribution of carbonate facies over an area of 6000 km² in the Red Sea.

By simulating carbonate layers using computer-modelled successions generated by non-random sea-level changes, Dexter *et al.* (2009) explored how a periodic sea-level signal propagates into the thickness distribution of stacked beds. While it might be expected that the bed thicknesses deposited under periodic sea-level fluctuations would be deterministic, Dexter *et al.* (2009) instead show this only to be the case when sea-level fluctuations are of particularly high-magnitude; for all other scenarios, the distributions: "are difficult to distinguish from random". Also using a computer model, Burgess & Pollitt (2012) similarly show how lithofacies with thicknesses that are inseparable from random can be generated under periodic fluctuations in sea-level. Comparable simulations conducted by Burgess (2006) and Hill *et al.* (2012) delivered the same result. The message that can be taken from these modelling exercises is that shallow-water sequences in the rock

record may appear random, even if deposited under non-random oscillations of sea-level. Through mathematical treatment of real-world data, Wilkinson *et al.* (1996) was unable to reject randomness as the most plausible explanation for the stacking patterns of lithofacies that presumably were laid down under periodic sea-level oscillation, and went as far as to suggest that: "meter-scale cyclicity in many if not most epicratonic sequences is more apparent than real". The results are profound and suggest that the perceptions of repeated and eustatically driven platform flooding, as would be suggested by sequence stratigraphic analysis, may be largely incorrect. Instead, Wilkinson *et al.* (1996) postulate that the metre-scale order recognized in peritidal carbonates is unrelated to changes in water depth and reflects the random migration of various sedimentary subenvironments over specific platform localities during the long-term accumulation of peritidal carbonate, a notion supported by Diedrich & Wilkinson (1999). Under these auspices, the occurrence of different lithofacies is not diagnostic of palaeo-water depth. While accepting the variability of shifting loci of carbonate sedimentation and deposition, Osleger (1991), by contrast, assert it to be insufficient to explain the persistent lateral and vertical rhythmicity of Cambrian subtidal carbonate cycles that can be correlated from outcrops separated by tens of kilometres. In Cretaceous outcrops, Strasser (1988) similarly recognized that autogenic processes occur locally, but deemed them to be overprinted by drops in sea-level that affected the entire platform. The issue of autogenic versus allogenic control remains divisive.

Although the link to palaeo-water depth is fundamental to the interpretation of fossil carbonate strata, few studies provide quantitative data on modern facies and bathymetry. Of the studies that do, all have been conducted at limited spatial scales, are biased in number towards the tropical Atlantic, and yield results varying between randomness and determinism in the arrangement of lithofacies with respect to depth. For instance, Rankey (2004) examined 400 km² of seabed offshore of the Florida Keys with a depth range of 1 to 9 m and concluded there to be a random arrangement of facies with depth. Similarly, Wilkinson *et al.* (1999) concluded a random patterning for 723 000 km² of Florida-Bahamas facies in space; depth was not considered, but depositional topography in the study area is variable. In the Arabian Gulf, Purkis

et al. (2005) also failed to identify any correlation between facies type and water depth for a 25 km² plot in which facies were mapped for depths spanning 5 to 7 m. Neither was a correlation between facies and depth returned by Purkis *et al.* (2012a) for a study covering 9600 km² in the Red Sea. In this case though, the facies mapping was fairly coarse because it was conducted from Landsat which offers pixels of only 900 m². In contrast, by considering 2 km² of Florida seabed with water depths ranging from 0 to 3 m, Bosence (2008) employed embedded Markov chain analysis to identify that the relation of facies to depth is ordered. It should be noted that the Markov approach of Bosence (2008) is quite different from that of Rankey (2004) and Purkis *et al.* (2012b), who employed metrics to estimate the uncertainty in predicting the abundance of facies elements at different water depths. In a study from the Pacific covering an area of 65 km² with water depths spanning 0 to 40 m, Purkis & Vlaswinkel (2012) show several facies to inhabit narrow and well-defined depth regimes, sufficient to be considered non-random, whereas others could not be constrained so precisely.

Despite methodological differences, the status quo on the ordering of facies to water depth hence falls into three camps; a handful of studies that observe ordering that is indistinguishable from random (Rankey, 2004; Purkis *et al.*, 2005; Wilkinson *et al.*, 1996, 1999; Purkis *et al.*, 2012a), two studies that report deterministic ordering with respect to depth (Bosence, 2008; Maloof & Grotzinger, 2012) and one study that shows aspects of both randomness and determinism (Purkis & Vlaswinkel, 2012). Interestingly, the two cases which provide evidence for depth-indicative facies (Bosence, 2008; Maloof & Grotzinger, 2012) come from situations where rates of sediment accumulation have been sufficiently rapid to build carbonate sequences that reach sea-level and above.

The present study differs from those that have preceded it by covering a large area (6000 km²) at high spatial resolution (4 m) over a substantial range in water depth (0 to 40 m). This difference in scope, combined with new statistical assessment, should provide fresh insight into a classic question in carbonate stratigraphy. The aims of this study were three-fold:

1 To ascertain the degree of facies heterogeneity and substitutability that occurs within a series of small (1 m) depth ranges in the zone of

maximum carbonate production and across a gradient in hydrodynamic energy.

2 To explore relations between lateral facies extent, water depth and wave energy.

3 To gain insight from the arrangement of facies with respect to water depth and energy regime in the Modern ocean that is useful for interpreting how lithofacies in the rock record partition by environment of deposition.

FOCUS AREAS AND SETTING

Cutting NNW to SSE across a Precambrian shield, the Red Sea is an active rift system covering 20° of latitude. Rift spreading began in the late Oligocene and the basin evolved from a series of continental lacustrine depressions into the 2200 m deep marine trough of today. The clear tropical waters of the Red Sea support vigorous coral reef growth and associated production of carbonate sediment. Clear waters are also conducive to the examination of the photic sea floor using satellite remote sensing. Local fault networks related to the extensional tectonics of the rift basin have been shown to influence the depositional geometry of coral reefs in the Red Sea (Purkis *et al.*, 2012a), as has salt diapirism, karst dissolution and the spatially variable input of siliciclastic detritus onto the coastal shelf during sea-level lowstands (Purkis *et al.*, 2010; Rowlands *et al.*, 2014).

The present study considers two focus areas separated by 320 km on the Saudi Arabian coastline of the Red Sea (Fig. 2A). As for the rest of the basin, these areas are characterized by an almost uninterrupted belt of fringing reefs, as well as barrier reefs and atolls (Rowlands *et al.*, 2012). Climate is hyper-arid, although there have been episodes of palaeo-humidity as recent as the early Holocene, caused, in the southern Red Sea, by a northward migration of the Indian Ocean Monsoon (IOM) and in the north, by westerly winter rainfall originating in the Mediterranean (Arz *et al.*, 2003; Davies, 2006). Quaternary climate fluctuations have been evoked to explain fine-scale karst control of the patterning of reefal ridges for the two focus areas (Purkis *et al.*, 2010). Dominant winds blow from the northwest and are channelled by parallel mountain ranges that line the east and west margins of the Red Sea rift valley. The two focus areas consist of extensive shore-attached lagoons closed on their seaward margins by fully aggraded barrier

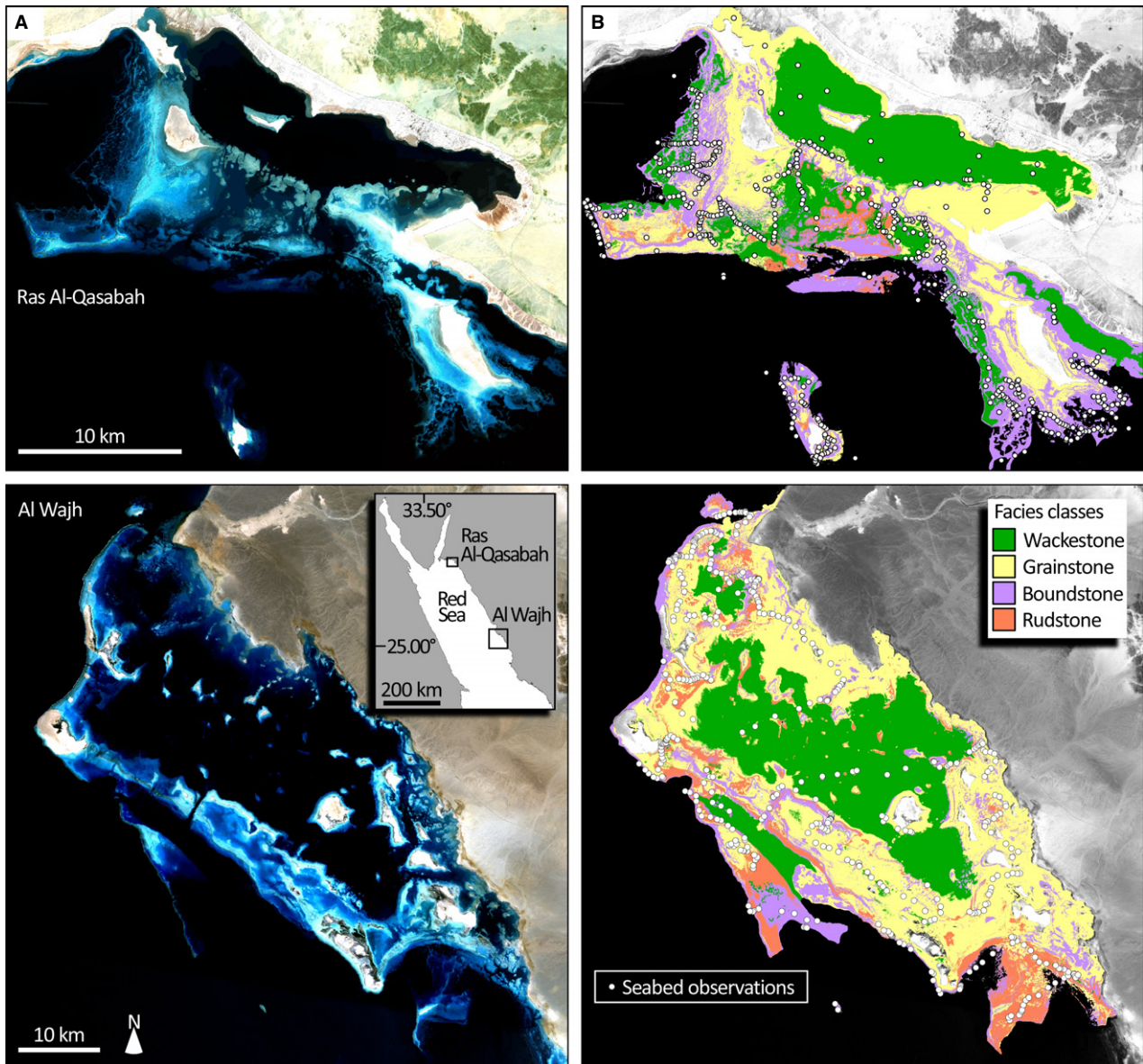


Fig. 2. Location of the two focus areas, Ras Al-Qasabah and Al Wajh, on the east coast of the Saudi Arabian Red Sea. QuickBird satellite imagery (DigitalGlobe Inc.) shows extensive coral reefs and associated carbonate sediments (blue to turquoise) rising out of deep water (black). Emergent sand cays and islands are tan to white. (A) Facies maps atop grey-scale satellite imagery. (B) Maps compiled by interpretation of satellite imagery guided by seabed observations (*white dots*). Note the scale change between focus areas.

reefs. This ‘rimmed shelf’ style of attached carbonate platform is assumed to have developed through large parts of the geological record with different producers but similar ecological niches and generally similar facies belts (Tucker, 1990; Handford & Loucks, 1993; Wright & Burchette, 1996; Pomar, 2001). The area of carbonate deposition for Ras Al-Qasabah covers *ca* 1000 km², which is considerably smaller than that of Al Wajh (*ca* 5000 km²).

METHODS

Facies maps

QuickBird multispectral satellite imagery (DigitalGlobe Inc., Longmont, CO, USA) was acquired for both focus areas concurrent to field visits. QuickBird imagery is composed of pixels with a 4 m side-length. The instrument collects across three water penetrating spectral bands (blue,

green and red) and a non-water penetrating infrared band that can be used to correct for atmospheric and sea-surface effects (such as sun glint). Fieldwork was spread over four campaigns conducted between 2006 and 2009 aboard the motor yacht *Golden Shadow*, a 67 m logistical support vessel. To aid interpretation of the satellite imagery, 600 videos of the seabed (200 Ras Al-Qasabah; 400 Al Wajh), each 30 sec in duration, were collected with a tethered 'drop' video camera interfaced with a differential GPS system and recorded digitally on a laptop computer. The tethered video observations were supplemented with snorkel and SCUBA dives, which were used to characterize the sea floor, including biota, physical and biological sedimentary structures, sediment type and other notable features. For each video and dive observation, the biotic composition of the sea floor was recorded and assigned to one of four rock-equivalent Dunham textures; wackestone, grainstone, boundstone or rudstone (Dunham, 1962; Embry & Klovan, 1971). The facies assignments were made on the basis of visual examination of the sediment and validated through the collection of samples at every tenth site. Collected samples were dried, sieved and inspected using a stereo binocular microscope. In this way, the reproducibility of the visual assignment of facies categories was assessed and the replicate analysis showed that the visual and quantitative methods differed in only 3% of cases. The approach was therefore deemed reliable. A facies map for each focus area was generated by pairing field observations constrained by differential GPS, with computer and manual interpretation of the QuickBird imagery. The duality that exists between biological habitats and depositional facies was recognized (following Rankey, 2004) and it was useful to cross-validate the evolving facies polygons against the habitat maps generated by Rowlands *et al.* (2012) for the same focus areas. The culmination of the mapping exercise was a matrix composed of $4\text{ m} \times 4\text{ m}$ pixels with facies assignments encoded with integer values (Fig. 2B).

Bathymetry models

Following the ratio-algorithm method of Stumpf *et al.* (2003), approximately four million single-beam depth soundings collected in the field (1.5×10^6 Ras Al-Qasabah; 2.5×10^6 Al Wajh) were used as training data. Spectral bathymetry was extracted from the QuickBird imagery. This empirical approach for extracting depth from

satellite data capitalizes on the differential attenuation of blue and green light by water. Because the green QuickBird band is attenuated more rapidly by water than the blue, it will always have lower reflectance values over submerged targets. Accordingly, as the image pixel values vary with water depth, the ratio between the blue and green bands will also change. As the depth increases, although the reflectance of both bands decreases, the reflectance of the band with the higher absorption (green) will decrease proportionally faster than the band with the lower absorption (blue). Hence, the ratio of the blue to the green band will increase. A ratio transform will also compensate implicitly for variable bottom type because changing seabed albedo affects both bands similarly, while changes in water depth affect the high absorption band more. Since this change in ratio due to depth is much greater than that caused by changes in bottom albedo (for example, sand versus coral reef), different bottom albedos at a constant depth will still have very similar ratios and therefore do not yield erroneous bathymetry estimates.

A digital elevation model (DEM), which captures seabed topography for water depths between the intertidal and 40 m, was calculated for each focus area. Complete attenuation of the QuickBird green channel prevents spectral derivation of depths ≥ 30 m. In order to extend the assessment of bathymetry down to 40 m, the limit to which facies were mapped, depths in the 30 to 40 m depth range were interpolated from a dense network of field-acquired single-beam soundings supplemented by points digitized from British and Saudi Admiralty charts. The spectrally derived depths were combined with those interpolated from soundings and charts to yield a seamless DEM for each focus area covering water depths ≤ 40 m with a spatial resolution of $4\text{ m} \times 4\text{ m}$ (Fig. 3A). Admiralty charts were used to assess the accuracy of the DEMs and a root mean squared error of 0.1 m was returned for depths ≤ 30 m. Accuracy of the 30 to 40 m depth range could not be assessed from Admiralty charts because they were partially used in the construction of the DEMs and were therefore not independent.

Wave height models

In a general overview, the main features of shallow-water hydrodynamics are wind waves, generated by the stress exerted on the ocean surface by the wind. Because long-period ocean

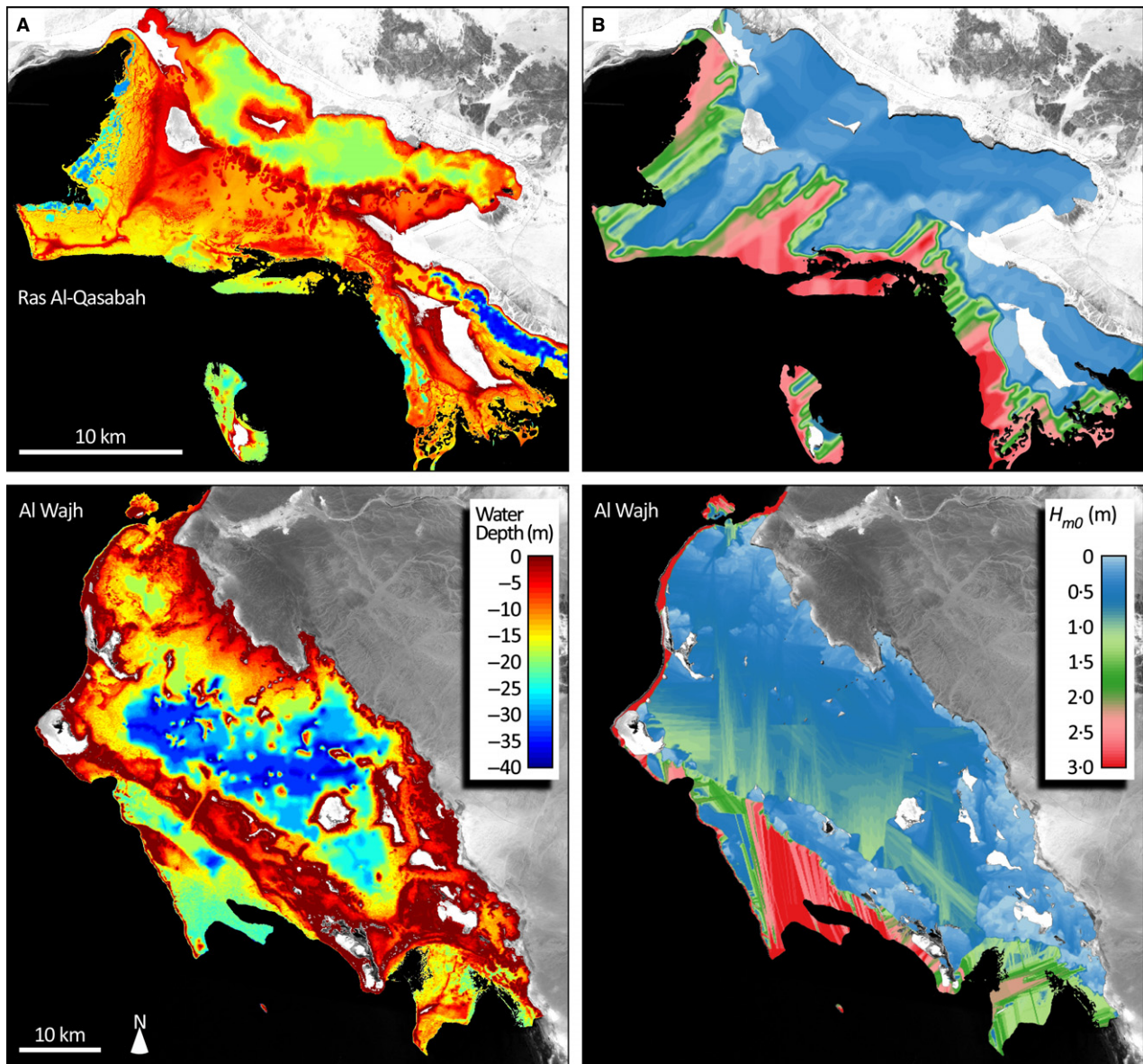


Fig. 3. Bathymetry models for the two focus areas, Ras Al-Qasabah and Al Wajh, atop grey-scale satellite imagery. (A) Water depth retrieved from the imagery via spectral modelling calibrated by field-acquired acoustic depth soundings. Models of significant wave height, H_{m0} , describe the mean of the 33% highest waves for the period 1999 to 2008 as predicted by the configuration of the coastline, bathymetry and regional meteorological conditions (see text for details). (B) In the Al Wajh lagoon, the linear green streaks corresponding to wave heights in the range of 1.0 to 1.5 m are created by the constructive interference of swell entering the lagoon through apertures in the reef rim.

swell transits from deep to shallower waters, waves are attenuated by energy dissipation through seabed friction. Eventually, the proximity of the seabed will cause the waves to break, producing a severe increase in the marine turbulence level and generating different types of currents which may extend beyond the surf zone. Control by wave exposure on the arrangement of coral frameworks and non-consolidated sedi-

ments have long been recognized in the modern ocean (Sheppard, 1982; Graus & Macintyre, 1989; Chollett & Mumby, 2012) and rock record (Allen, 1979; Sundquist, 1982; Wehrmann *et al.*, 2005; Immenhauser, 2009).

While *in situ* wave data were unavailable for the two focus areas, wave exposure can be calculated using cartographic indices within the framework of a Geographic Information

System (GIS), (Ekeboom *et al.*, 2003; Chollett & Mumby, 2012). The physical model of Rohweder *et al.* (2008) was used which, on the basis of the configuration of the coastline, bathymetry and regional meteorological conditions, delivers a spatially explicit (pixel-based) estimate of wave exposure. Wave height refers to the vertical distance between the highest and the lowest surface elevation in a wave. The term 'significant wave height', H_{m0} , refers to the mean of the 33% highest waves (Immenhauser, 2009) and was calculated for the two focus areas via:

$$H_{m0} = H^{\wedge}_{m0} \frac{(U_f)^2}{g} \quad (1)$$

where g is the acceleration of gravity (9.82 m sec^{-2}) and the friction velocity (U_f) was computed via:

$$U_f = (C_d)^{1/2} U_{\text{scat}} \quad (2)$$

where the coefficient of drag of wind against the sea surface (C_d) is expressed as:

$$C_d \approx 0.001 \times (1.1 + (0.035 \times U_{\text{scat}})) \quad (3)$$

with U_{scat} being the adjusted wind speed (m sec^{-1}) for the two focus areas as derived from QuikSCAT satellite scatterometer data for the period 1999 to 2008, downloaded on 1 August 2013 from www.ssmi.com/qscat/. Wind data, originally at 15 km spatial resolution, were interpolated to 100 m prior to the analyses. The non-dimensional significant wave height (H^{\wedge}_{m0}) was computed according to:

$$H^{\wedge}_{m0} = 0.0413(x^{\Delta})^{1/2} \quad (4)$$

where the non-dimensional wind fetch (X^{Δ}) is defined as:

$$X^{\Delta} = \frac{(g \times x)}{(U_f)^2} \quad (5)$$

x is the pixel-based wind fetch (m) in 36 compass directions calculated following Chollett & Mumby (2012). In this step, fetch is calculated from a base map for the Red Sea that captures the position of emergent features as well as submerged areas that reach within 3 m of the sea surface, as defined by digitized British and Saudi admiralty charts and manual interpretation of Landsat imagery. The raster layers of H_{m0} were up-scaled to the resolution of the facies and bathymetric maps for the two focus areas ($4 \text{ m} \times 4 \text{ m}$) and have pixel units of metres (Fig. 3B).

Facies entropy and the Akaike information criterion

The three data layers (facies type, water depth and wave height) were assembled in a GIS for statistical treatment. To identify trends, a standard is needed against which to judge whether the tendency for a particular facies to associate with a water depth or energy regime (or range in these variables) is greater or less than random. To this end, Rankey (2004) employed the maximum entropy concept whereby divergence from a state of disorder is statistically assessed. When considering depth, the end-members to this approach are perfect determinism – one water depth, one facies – and randomness, where the depth arrangement of a number of facies exhibits a state of maximum disorder (water depth and facies are independent). The same principle can be applied to assess how facies stratify with respect to wave energy. To explore trends within these data, the Shannon evenness index was used to examine facies diversity (substitutability) across the range of water depths and wave heights recorded for the two focus areas (Shannon, 1948; Rankey, 2004).

Described here for water depth ranges, but equally calculated for wave height ranges, the calculation proceeds as follows. Given a water depth range in which there exist n possible facies classes, with proportions p_1, \dots, p_n within that water depth range, evenness (E) for each water depth is calculated as:

$$E = 1 - \frac{-\sum_{i=1}^n p_i \cdot \ln p_i}{\ln(n)} \quad (6)$$

To implement Eq. 6, bathymetry was partitioned into 1 m bins spanning 0 to 40 m. Wave height, conversely, was split into 30 bins, each spanning 0.1 m, to cover the range of wave heights computed for the two focus areas (0 to 3 m). To ensure representative sampling, E was not computed for depth or wave height bins containing fewer than 1000 observations. Evenness (E) scales from zero to one, with values near unity showing that a bin of water depth or wave height is not diverse, but instead dominated by one facies class. In this situation, there is a more deterministic relation; given a water depth (or wave height), the facies present can be predicted with confidence (Rankey, 2004). Under such conditions, by looking at a

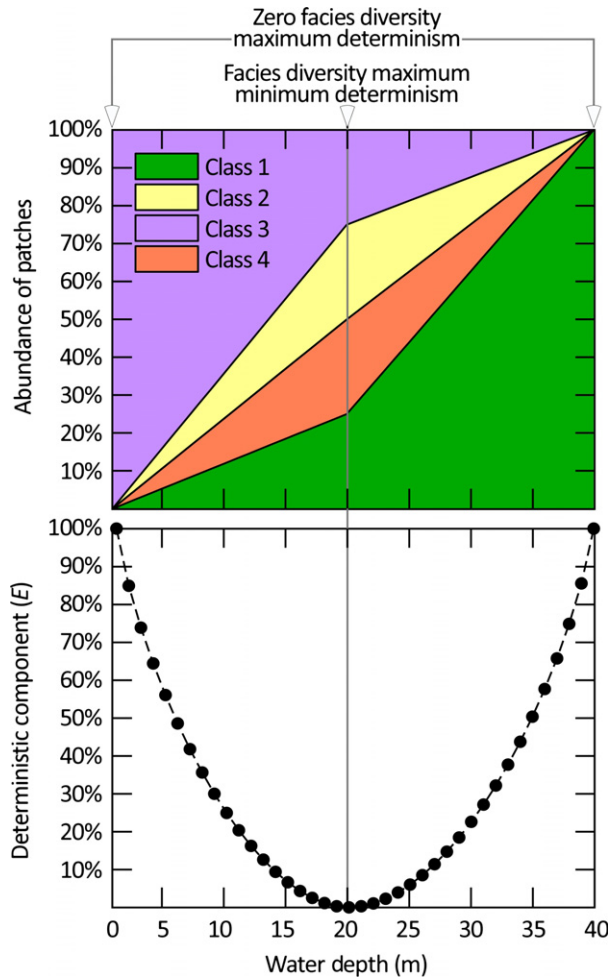


Fig. 4. An example using synthetic data to illustrate the behaviour of the Shannon evenness index (E) with varying proportions of four classes over 40 depth bins (calculated using successive implementation of Eq. 6). Class 3 accounts for 100% of occupancy at 0 m water depth; there is therefore no diversity in occupancy and the relation between depth and class occurrence is completely deterministic. The situation is the same for Class 1 at 40 m depth. At 20 m depth, however, there is 25% occupancy for each of the four classes which represents the maximum possible level of diversity between the four classes and therefore minimum intensity of determinism ($E = 0\%$).

map of facies, a map of depth could be inferred, or vice versa. Evenness (E) equals zero for the situation where a depth or wave height bin is occupied by an equal proportion of all four facies classes (wackestone, grainstone, rudstone and boundstone) – the case of maximum entropy, and E equals one for which the knowledge of water depth (or wave height) carries the least predictive power for facies class (see four class example with synthetic data, Fig. 4).

Between zero and one, E is proportional to the percentage that uncertainty has been reduced from the maximum. For example, as described by Rankey (2004): “for a given water depth, a value of $E = 0.20$ means that the observed uncertainty in class occurrence has been reduced 20% relative to the maximum possible entropy and, conversely, that there is a 20% deterministic or predictable component, as constrained by water depth”. The relative contribution of the facies classes to each water depth and wave height bin was computed in order to develop stacked area graphs. Trends in E with respect to water depth and wave height were evaluated through scatter plots (Figs 5 and 6). Size-frequency relations for facies bodies and the connection between patch size, water depth and wave height were examined using log-log cumulative distribution plots (Figs 7 and 8).

The next tier of the analysis employs an information-theoretical approach based on the Akaike information criterion (AIC), a measure of the relative goodness of fit of a statistical model (Akaike, 1973). Like Shannon evenness, the AIC is grounded in the concept of information entropy, which offers a relative measure of the information gained as explanatory variables are added to a predictive model. The approach also allows multiple candidate models to be compared simultaneously. The AIC is therefore suitable to simultaneously investigate the descriptive power of multiple models that combine water depth and wave energy to forecast sediment character.

The AIC is employed to rank the ability of four competing candidate models (Table 1) to predict facies category. Each model represents a competing hypothesis for factors controlling facies occurrence. Since the response variable, facies, is a discrete classification, a logistical model (Eq. 7) is used to describe the presence or absence of each facies category at each pixel in the facies map as a function of water depth (wd) and/or significant wave height (H_{m0}), via:

$$\text{logit}^{-1}(-x) = \frac{1}{1 + \exp(-x)} \quad (7)$$

where x is an explanatory variable (for example, wd , H_{m0} or a combination of the two). For each model, the AIC weight, w_i , is calculated to quantify the evidence supporting each model as the best of the four proposed (Burnham & Anderson, 2002). The models were ranked on the basis of w_i , which scales 0 to 100%, to identify the combination of explanatory variables that provides

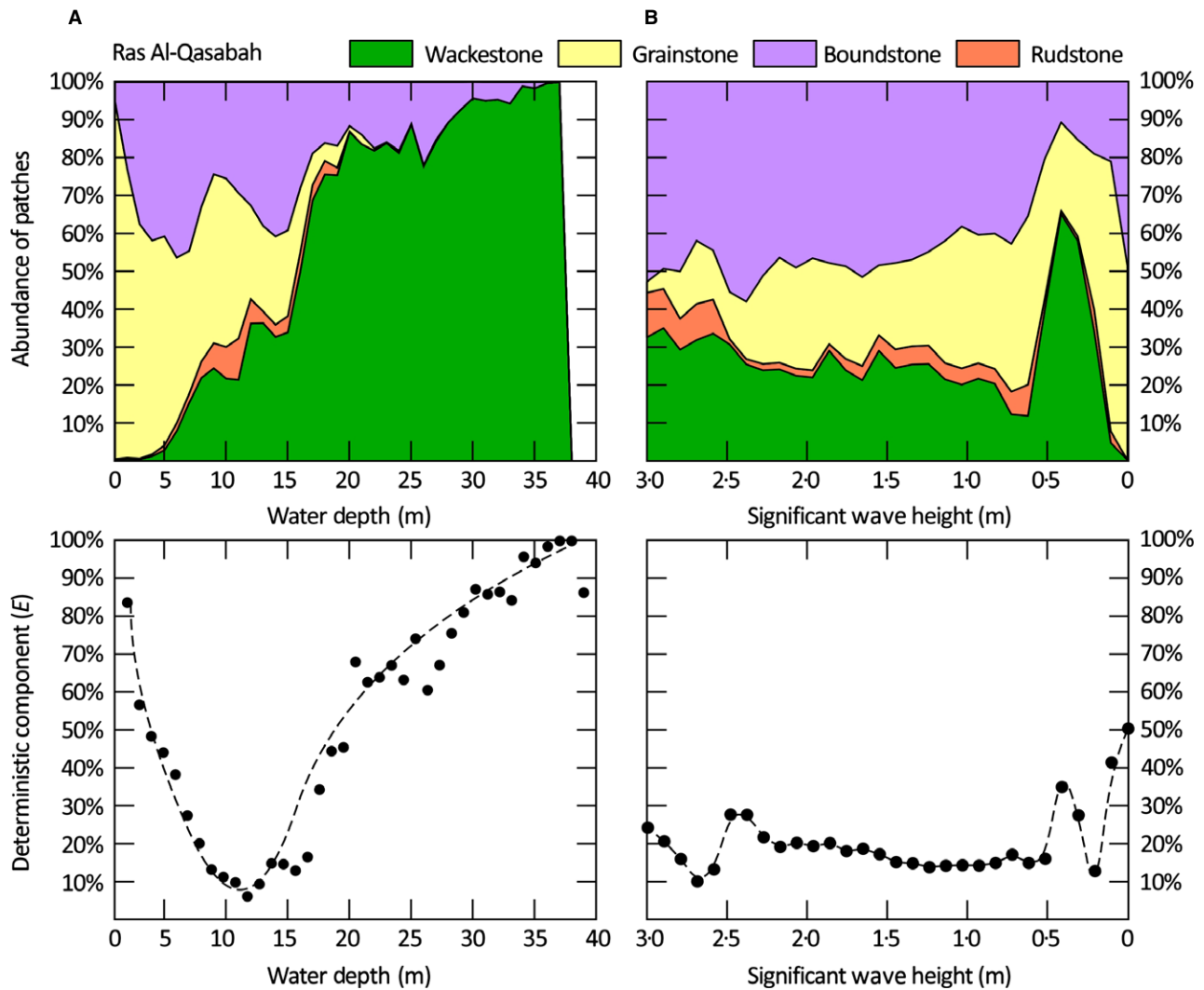


Fig. 5. Ras Al-Qasabah. (A) Plots the abundance of facies patches (%) for each water depth (top) and Shannon evenness (E) characteristics of facies as related to water depth (bottom). (B) Plots the abundance of facies patches (%) for each significant wave height (top) and E characteristics of facies as related to wave height (bottom).

the most reliable prediction of facies category. The model with the highest w_i is considered the best fit. The comparison was performed using the R statistical program (R Development Core Team, 2008).

All four candidate models include a term to account for the fact that the lateral distribution of facies is spatially autocorrelated. Spatial autocorrelation occurs when an observation at one location either positively or negatively affects the observation at another point (Legendre, 1993). For instance, adjacent pixels in the facies map have a higher probability of being classified as a common facies category than those separated more widely (Purkis & Vlaswinkel, 2012). This phenomenon must be accounted for to

reduce bias within the results. Standard procedure (e.g. Augustin *et al.*, 1996) was followed and a correlogram was developed for each facies category, which plots distance between a pair of pixel coordinates (x -axis) against correlation (y -axis). An exponential model is fitted to the correlogram and used to provide a spatial autocorrelation value, sac , for each observation, which is included in the four candidate models (Table 1).

Since the two focus areas provide millions of postings for facies, water depth and wave height (Ras Al-Qasabah 5.2 million, Al Wajh 30 million), computation of spatial autocorrelation for every observation was impractically time-consuming. Therefore, an iterative strategy of sub-setting the data was adopted whereby

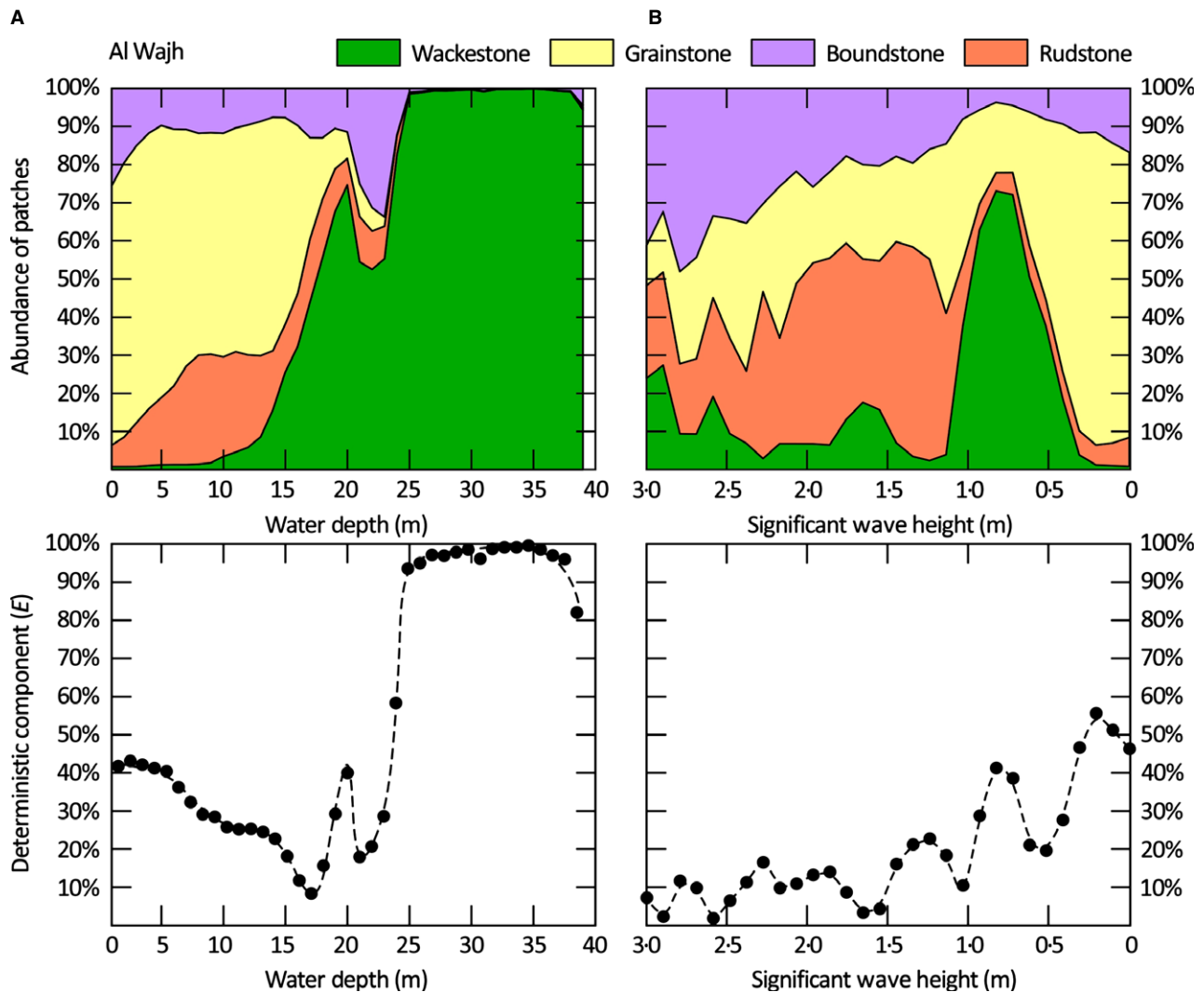


Fig. 6. Al Wajh. (A) Plots the abundance of facies patches (%) for each water depth (top) and Shannon evenness (E) characteristics of facies as related to water depth (bottom). (B) Plots the abundance of facies patches (%) for each significant wave height (top) and E characteristics of facies as related to wave height (bottom).

10 000 observations were extracted randomly from the full dataset and the model comparison conducted. This process was repeated 100 times for each focus area.

Is the occurrence of a facies diagnostic of a range of depositional water depths?

While the facies entropy and AIC calculations describe how facies textures are controlled by depth and waves, it is not permissible to recast the results to inform how diagnostic the occurrence of a particular facies is for a given water depth (or range in depths), as would be useful for the interpretation of lithofacies in a stratigraphic sequence. To access this informa-

tion, cumulative probability curves for each facies were calculated for binned depth values using the following routine. Firstly, an equal number of points (100 000) were randomly selected from the GIS maps of Ras Al-Qasabah and Al Wajh to yield 200 000 coincident measurements of facies texture and water depth. Secondly, the number of occurrences for each facies was tallied for eight depth bins, each 5 m wide, spanning the range of 0 to 40 m. Thirdly, the occurrence tallies were assembled into a cumulative probability function for each facies. Fourthly, the three-step procedure was repeated 1000 times and the results were averaged and graphed (Fig. 9A). A hypothetical case study was then developed to illustrate how lithofacies

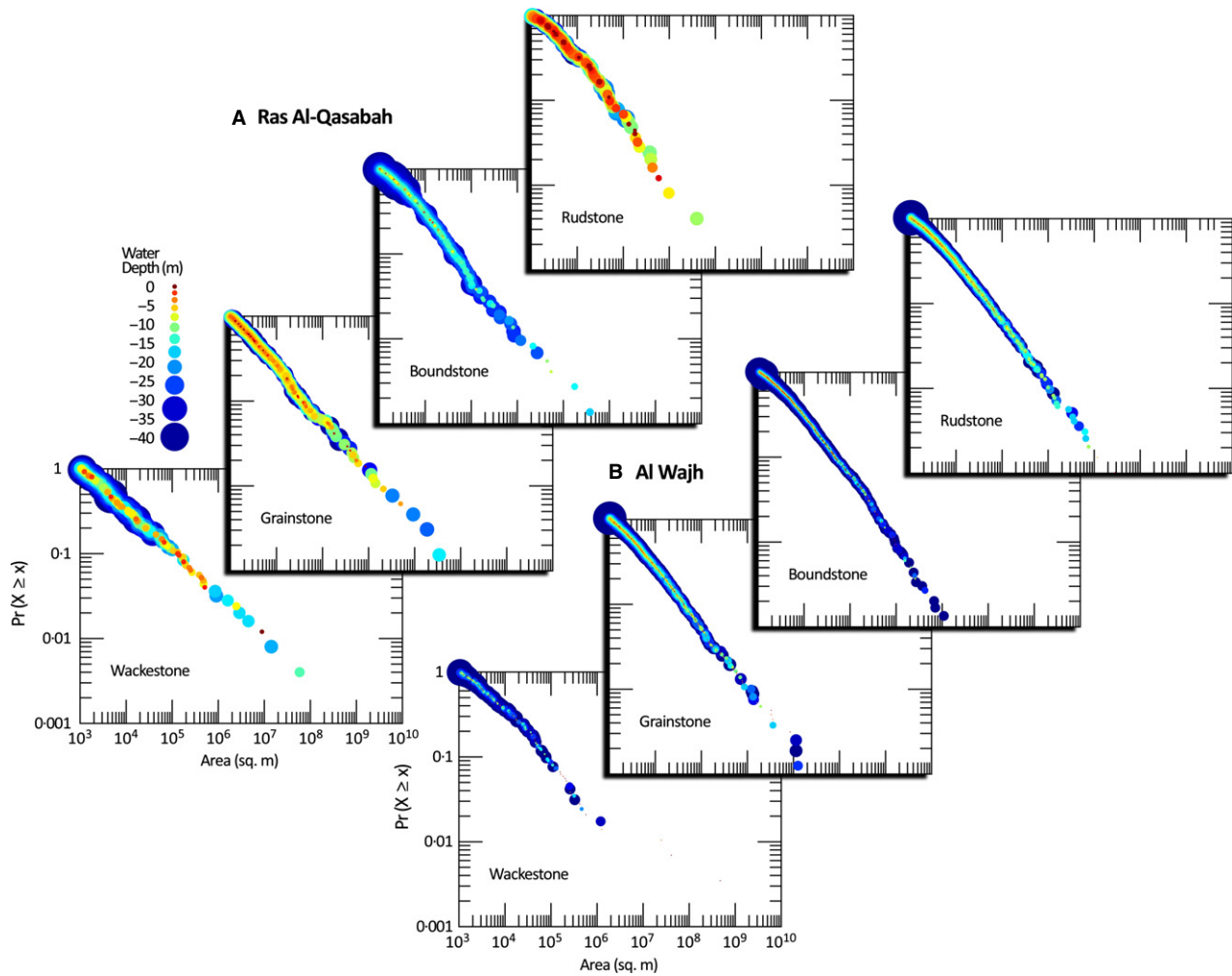


Fig. 7. Cumulative distribution functions for the rock-equivalent Dunham textures mapped in Ras Al-Qasabah (A) and Al Wajh (B): x-axis – log facies body area, y-axis – log probability of encounter $P(X \geq x)$. Straight-line trend throughout each population indicates power-law relations, upheld by the statistical test of Clauset *et al.* (2009). Median water depth for each facies body is indicated by marker size and colour. No systematic relation between depth and body area is evident.

in a subtidal carbonate sequence might be interpreted in the light of the calculated Red Sea facies-depth distributions (Fig. 9B). The purpose of this hypothetical exercise was to illustrate potential pitfalls in hindcasting palaeo-water depth from the physical rock record.

RESULTS

Spatial patterns in geomorphology, sedimentology and hydrodynamics of the focus areas

The lateral relations between geomorphology, facies, bathymetry and wave height can be

explored in the satellite imagery and its derivatives. Water depth maps show only small portions of each focus area to be fully aggraded to sea-level (2% of Ras Al-Qasabah is built to the low-tide datum; 20% of Al Wajh). If transferred to the rock record in their current configuration, both systems would be dominated in area by subtidal carbonate strata with only rare occurrences of peritidal strata topped with exposure surfaces.

For both focus areas, facies tend to be more continuous along strike and more apt to change along dip. The fact that gradients in both water depth and wave energy are broadly dip-orientated is undoubtedly relevant to this patterning (a premise explored numerically by Purkis &

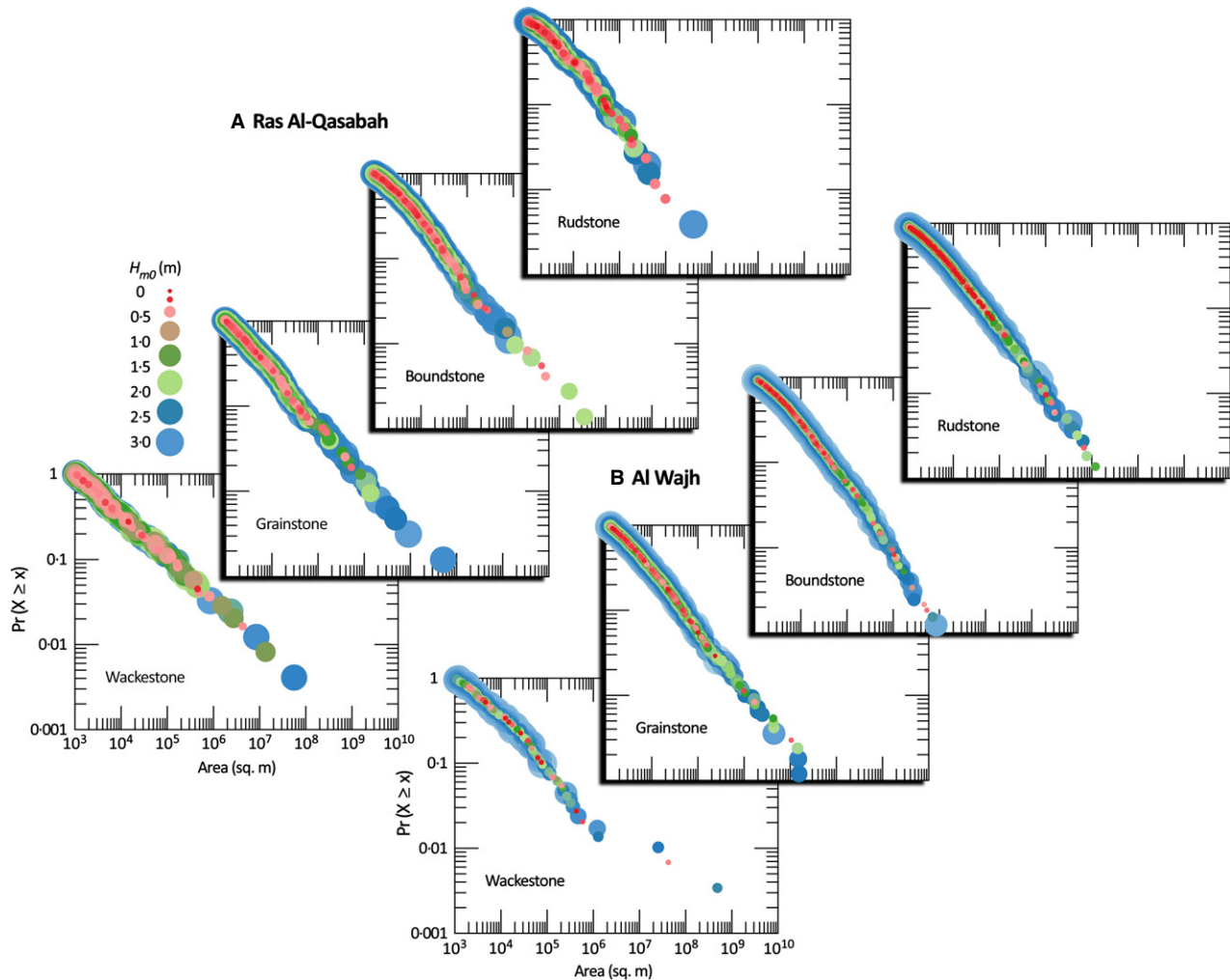


Fig. 8. Cumulative distribution functions for the rock-equivalent Dunham textures mapped in Ras Al-Qasabah (A) and Al Wajh (B). Median significant wave height (H_{m0}) for each facies body is indicated by marker size and colour. As for water depth, no systematic relation between wave height and body area is evident.

Table 1. Definition of the four competing models considered using the Akaike information criterion (AIC).

Model name	Model
Water depth only	$\Pr(Y_i = 1) = \text{logit}^{-1}(\beta_0 + \beta_s \cdot \text{sac} + \beta_{wd} \cdot wd)$
Wave height only	$\Pr(Y_i = 1) = \text{logit}^{-1}(\beta_0 + \beta_s \cdot \text{sac} + \beta_{H_{m0}} \cdot H_{m0})$
Water depth + wave height	$\Pr(Y_i = 1) = \text{logit}^{-1}(\beta_0 + \beta_s \cdot \text{sac} + \beta_{wd} \cdot wd + \beta_{H_{m0}} \cdot H_{m0})$
Random	$\Pr(Y_i = 1) = \text{logit}^{-1}(\beta_0 + \beta_s \cdot \text{sac})$

sac = spatial autocorrelation value; wd = water depth (m); H_{m0} = significant wave height (m) and $\text{lit}^{-1}(x)$ is the logistic function of x .

Vlaswinkel, 2012). Al Wajh possesses a well-developed reef crest, at or near low-tide sea-level, bordering the shelf margin. Maps of signifi-

cant wave height show this rimmed platform to be dominated by low-energy conditions because open-ocean swells rapidly lose energy crossing

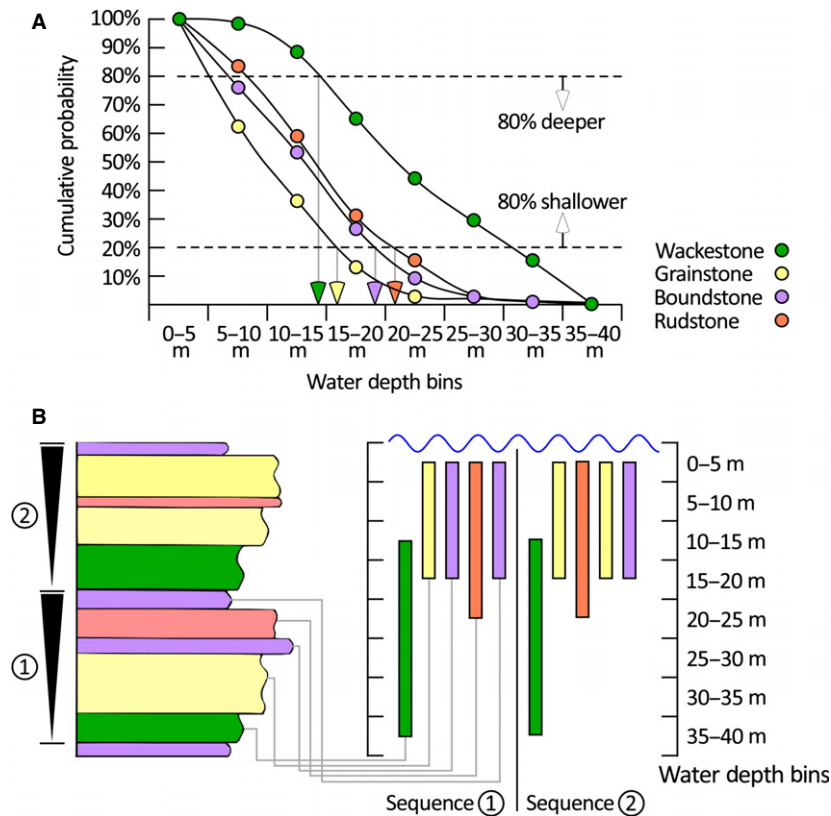


Fig. 9. (A) Plots the cumulative probability (y-axis) that each facies occurs within a given depth bin or deeper (x-axis) as derived from the facies and depth maps for Ras Al-Qasabah and Al Wajh. Depth bins are 5 m wide and span the range of 0 to 40 m. (B) Highlights the implication of the facies-depth trends identified in (A) for interpreting two hypothetical subtidal parasequences. Taking an 80% level of confidence [bounded by the *horizontal broken lines* in (A)], two possibilities are presented for the position of sea-level through deposition of the two parasequences. Firstly, that at the base of the parasequence, the occurrence of wackestone indicates water depths greater than 10 m, which shallow to less than 20 m for the deposition of the beds of grainstone, rudstone and boundstone. Secondly, and equally probable, both parasequences could have been deposited under a water depth of 10 to 15 m and a static sea-level (all facies occur within this depth range). Using the Red Sea data as an analogue, with an 80% level of confidence, it cannot be unequivocally stated that the hypothetical subtidal sequences are upward shallowing.

the protective reef rim. A grainstone apron is best developed shoreward of the rim and fine-grained (wackestone) sediments accumulate within the large restricted subtidal lagoon. Although Ras Al-Qasabah also holds a fully aggraded reef rim, unlike Al Wajh, it is offset from the shelf-edge and serves to segregate locally the depositional system along strike into two halves. Abundant patch reefs (primary boundstone) occupy the sector seaward of the rim and grow to near sea-level, delivering a complex arrangement of geomorphology and wave regime. Topography is a primary driver of facies change in this area. As for Al Wajh, the sector shoreward of the rim takes the form of a >20 m deep lagoon infilled with fine-grained sediments. In Ras Al-Qasabah, as in

Al Wajh, it can be assumed that offbank sediment transport is considerably reduced by the platform-edge reef barrier.

For both focus areas, some broad trends are immediately obvious between the GIS data layers. For instance, areas mapped as boundstone predominantly correspond to water depths <5 m and display the highest significant wave height, although there are exceptions. Lagoon floors of both focus areas are wackestone-dominated, of deep water depth and, by virtue of the shelter provided by the reefal rims that separate the lagoons from the open ocean, are of low significant wave height. Further trends and patterns in the data are revealed through statistical examination.

Facies entropy varies with water depth and wave height

Following Rankey (2004), these data can be examined in terms of facies diversity as a function of water depth and significant wave height. Clear stratification exists between facies occurrence and water depth for Ras Al-Qasabah (Fig. 5A); grainstone and boundstone are indicative of water depths <5 m and wackestone dominates the sea floor at depths >20 m. Relations between E and depth reveal a more subtle trend, however. While the deterministic component is high in shallow and deep water, it is low at intermediate depths. For instance, for depths in the range of 0 to 5 m, uncertainty in facies character is reduced by 80% relative to the situation of maximum entropy (when all facies have an equal probability of occurrence). The same, or higher, levels of predictability exist for water depths >25 m. By contrast, for depths in the range of 5 to 25 m, the deterministic component is <50% (as low as 10% at 12 m water depth). In other words, with knowledge of depth in the 5 to 25 m range, facies can only be predicted 50% better than the situation of maximum entropy. At 12 m, facies can only be predicted 10% better than the equiprobable situation. Following the reasoning of Rankey (2004), facies deposited at intermediate water depths are not significantly differentiated or limited, while those deposited in shallow and deep water are differentiated. This situation is mimicked in Al Wajh where facies diversity is high at intermediate water depths, but decreases in the shallow and the deep (Fig. 6A). The degree of determinism in the depth range of 0 to 5 m for Al Wajh (40%) is half that of Al-Qasabah, however. This difference in predictability occurs because of the prevalence of rudstone in the shallow debris apron of Al Wajh that lies shoreward of the reef rim, along with extensive deposits of grainstone and boundstone.

For Ras Al-Qasabah and Al Wajh, facies diversity with H_{m0} follows a different pattern than observed for water depth. At both sites, facies do not behave conservatively with respect to hydrodynamic energy and the situation of maximum entropy is approached for all significant wave heights. The deterministic component is in the realm of 30% for H_{m0} spanning 0 to 3 m and, therefore, with knowledge of wave height, there is a slim chance that the correct facies could be predicted (Figs 5B and 6B).

It is important to note that the fluctuation of E is dependent on the number of facies defined

and therefore direct comparisons between studies employing the same metric, but a different number of mapped facies, can be misleading. More defined facies are likely to deliver less deterministic relations because, if the sediments are divided into more categories (for example, by further partitioning grainstone on the basis of the relative abundances of constituent particles), it is more likely that, for example, in the 0 to 5 m depth range, there will be numerous facies represented. Also note, however, that in this study and that of Rankey (2004), a small number of facies categories (four to five) are adopted. This number reflects the current ability of multi-spectral satellite remote sensing to discriminate between submerged sediment types.

Akaike information criterion model ranking

While Shannon evenness provides insight into trends of facies diversity across the range of water depths and wave heights recorded for the two focus areas, it is impossible with this index to assess simultaneously the combined effect of the two variables. Therefore, the AIC was employed to examine whether the combined effects of depth and wave height better predict facies occurrence.

For Ras Al-Qasabah, in every iteration of the model comparison and for three of the four facies categories (wackestone, grainstone and boundstone), the model that incorporates water depth plus wave height is ranked highest based on AIC. The fourth category, rudstone, is best predicted by the water depth plus wave height model in 85 of the 100 iterations and by wave height only for the remaining 15 iterations. For this facies, wave height is the variable common to the selected models, suggesting that waves are the dominant factor dictating the placement of rudstone in Ras Al-Qasabah. This said, rudstone is comparatively rare in the focus area (occupying only 30 km² of the 900 km² or 3% of the seabed mapped). Therefore, the model comparison contains greater uncertainty than the comparisons for the other three, more prevalent, facies categories. The results for Al Wajh are more straightforward. Here, in every iteration of the model comparison and for all four facies categories, the model that incorporates water depth plus wave height was ranked highest based on AIC weight (and $w_i = 100\%$ in all instances). These results support a single hypothesis for both focus areas; a combination of water depth and wave height is a better predictor of facies

category than either of the two variables considered individually.

Lateral facies extent is unrelated to water depth and wave height

Trends that might exist between the lateral continuity of sedimentary bodies and water depth can be investigated through a comparative analysis of the facies and bathymetry maps. If trends exist, they might offer useful insight into the horizontal extent of lithofacies in the rock record, information that is notoriously hard to gather because the lateral dimension of buried carbonate systems tends to be vastly undersampled with respect to the vertical dimension in outcrop and core.

For the two focus areas and for each of the four facies categories (wackestone, grainstone, boundstone and rudstone), each facies polygon was selected in turn and its area and median water depth extracted. Cumulative distribution functions, colour-coded by water depth, were then generated to simultaneously explore the size-frequency distribution of the facies bodies and size to depth relations (Fig. 7). The relation between facies extent and significant wave height was explored in the same way, but with median H_{m0} extracted per facies polygon instead of water depth (Fig. 8). For Ras Al-Qasabah and Al Wajh, neither was a systematic relation observed between water depth and lateral facies extent across the four facies categories, nor between wave height and extent. Interpreted in the context of the rock record, these results imply that lithofacies do not have a tendency to become laterally more continuous when deposited in deep or tranquil settings, over the range of depths and wave heights examined by this study. However, power laws characterize the size-frequency distributions of facies bodies mapped in both focus areas, as indicated by near-linear trends and by the test of Clauset *et al.* (2009).

DISCUSSION

Shallow-water carbonate facies do not precisely record water depth

The sequence stratigraphic concept for carbonates relies on the following assumptions. Firstly, that carbonate facies are controlled by water depth of deposition and, secondly, that a

water depth history can be inferred from ancient strata because of this. Thirdly, that apparent trends in water depth derived from such an interpretation are indicative of sea-level changes and therefore allogenic forcing of carbonate accumulation and, fourthly, that this allows identification of cyclicity in carbonate strata on the scale of a metre to a few metres. Indeed, this concept is partially supported by the data assembled in the Red Sea; the broad trend for both focus areas when comparing facies in 5 m water depth with those in 40 m water depth is a transition in dominance from grainstone and boundstone to wackestone, with increasing depth. These results suggest that for large excursions of sea-level, such as witnessed during ice-house settings, it might be anticipated that the depositional consequences will be recorded as a transition from wackestone to grainstone and boundstone. By contrast, lower amplitude sea-level fluctuations may remain undetectable based on facies.

When facies entropy with depth is considered statistically, however, the trend is more complicated. For instance, while the Shannon index reports facies substitutability to be low at shallow and deep water depths, it is high in the 5 to 25 m depth range, to the point that facies type can only be predicted 50% better than the situation of maximum entropy; from the perspective of the rock record, poor odds that a particular facies could be used to infer deposition in this depth range. By expanding the analysis to include the lateral distribution of wave height across the two focus areas, variations in hydrodynamic energy, arguably an autogenic process, are shown also to hold statistical power for the prediction of facies type, albeit less power than for depth. These results suggest the depositional texture of the studied sediments to be simultaneously controlled by an allogenic and an autogenic process in water depths shallower than 40 m.

Hindcasting palaeo-water depth from the physical rock record can be challenging for photic zone carbonates

The blend of influence from extra-platform and intra-platform processes was explored by creating four competing candidate models that were tested for their ability to describe the presence or absence of the four facies categories at each pixel in the two facies maps, as a function of water depth and/or significant wave height. The AIC was used to rank the ability of each model

to predict facies category, and it was unambiguously found that the model that simultaneously considered depth and wave height carried the most predictive power for all facies. The AIC results add further weight to the dual relevance of both allogenic and autogenic processes in explaining the complex patchy lateral facies mosaics evident atop modern carbonate platforms (Riegl & Piller, 1999; Purdy & Gischler, 2003; Purkis *et al.*, 2005; Andréfouët *et al.*, 2009; Rankey *et al.*, 2009; Reijmer *et al.*, 2009; Purkis & Vlaswinkel, 2012; Gischler *et al.*, 2013), as well as ancient carbonate platforms (Strasser, 1991; Grötsch & Mercadier, 1999; Strasser *et al.*, 1999; Weber *et al.*, 2003; Fournier *et al.*, 2005; Kenter *et al.*, 2006; Verwer *et al.*, 2009).

For someone who spends time in coral reef environments, the finding that facies character in modern platform-top carbonates is controlled dually by water depth and hydrodynamics might not come as much of a surprise. The real relevance of the study lies instead in the interpretation of subtidal lithofacies in the sedimentary record, where the complex interactions of the biological and physical components of a depositional system are erased by fossilization. Despite the loss of these cues, it remains necessary to solve patterns of water depth from lithofacies textures in order to reconstruct platform geometry and cyclicity and to place a carbonate system into a sequence stratigraphic framework. By constructing a test which places facies as the predictive variable for depth, it is possible to examine the confidence with which palaeo-water depth can be inferred from examination of ancient strata. On the basis of the cumulative probability distributions calculated for the two focus areas (Fig. 9A), with 80% confidence, it can be said that an occurrence of wackestone in the facies map coincides with a water depth of 10 m or greater. Conversely, grainstone and boundstone can be assumed to have been deposited in water depths of 15 m or shallower, with the same level of confidence. Rudstone appears in water depths shallower than 25 m in 80% of its occurrence. Using the Red Sea data as an analogue, it cannot be unequivocally stated that the hypothetical subtidal sequences are upward shallowing with an 80% confidence interval (Fig. 9B). Only with 70% confidence can it be postured that wackestone was deposited in deeper water than the grainstone, boundstone and rudstone. Casting these results in terms of a hypothetical subtidal

carbonate sequence, which is a common motif in the geological record for carbonate platform tops (Markello & Read, 1982; Aigner, 1985; Calvet & Tucker, 1988; Osleger, 1991), it is possible to emphasize how the mapped facies are not significantly differentiated or limited by water depth. The implication of the exercise is that a geologist faced with a metre-scale stack of subtidal lithofacies which coarsen upwards, cannot confidently infer shallowing. Under such auspices, identification of subtidal metre-scale carbonate cycles in the rock record poses challenges and appropriate caution should be applied during interpretation. Inferring sea-level fluctuations from peritidal facies remains a safer proposition because of the existence of clear sequence boundaries (subtidal facies sub-aerially exposed) and/or intertidal and supratidal facies, all of which are unequivocal indicators of a relative change in water depth. On the basis of the work of Wilkinson *et al.* (1996) and Diedrich & Wilkinson (1999), however, there remains scope for the misinterpretation of peritidal sequences.

Deviation from simple depth-controlled facies deposition has been suggested by many (Osleger, 1991; Strasser, 1991; Wilkinson *et al.*, 1996; Rankey, 2004; Purkis *et al.*, 2005; Wright & Burgess, 2005), but this article adds to the discussion in two ways. Firstly, this study offers numeric insight into the degree to which the elements of a facies mosaic are depth-dependent. Secondly, the observations from the study are derived at high resolution (metre-scale) and over a much larger area of seabed than has been examined previously (6000 km²), while retaining rigorous ground-control on both facies distribution and bathymetry. While the Red Sea data are informative, further testing in alternative modern settings is encouraged and it is hoped that this article will stimulate others to conduct work in the same vein.

This is not to say that this study is without weakness and bias. For instance, the employed rock-equivalent Dunham textures are insensitive to the full range of sedimentological parameters that can be used to tie facies to specific water depths. The class 'grainstone', for example, might be split into multiple subcategories on the basis of bedforms, sedimentary structures and the relative abundances of constituent particles (e.g. Ginsburg, 1956), as well as taphonomical, biological or chemical observations (Immenhauser, 2009). Similarly, 'boundstone' could be further partitioned by the growth form

or species compliment of corals. However, as previously noted, a more detailed sediment classification is likely to increase the level of facies substitutability with depth. It is also prudent to note that the two Red Sea focus areas, Ras Al-Qasabah in particular, are topographically more complex than many isolated platforms and rimmed shelves, although the findings of this study are in line with those from carbonate depositional environments with more modest bathymetric variation (e.g. Wilkinson & Drummond, 2004). Finally, if results from this study are to be considered as relevant to interpreting lithofacies arrangements in the rock record, it must of course be recognized that observations from the modern oceans are not *a priori* applicable to fossil ones. This said, while aspects of the biology of carbonate producers have changed through geological time, the physics of the carbonate system has not.

Lateral facies extents are unrelated to water depth

Beyond describing how facies type is dependent on water depth and wave energy, this study also presents findings on the lateral continuity of facies bodies with regard to these variables. The concept of ‘environments of deposition’ (EODs) is a useful way to group cross-platform associations of lithofacies deposited in similar water depths and hydrodynamic settings (Ginsburg, 1956). The concept is commonly applied because EODs can typically be recognized in cores, outcrops and aerial images alike. Systematic relations that might exist between lateral continuity of facies belts within an EOD would be exciting because they could be used to predict facies extent in outcrops and cores, where one or both of the lateral directions is unsampled, as investigated using Markov chains by Purkis *et al.* (2012b). Plots of lateral facies extent versus median depth and significant wave height for each facies body do not show strong trends (Figs 7 and 8), suggesting no tendency for facies bodies to be systematically larger or smaller in areas of deep water or backwater hydrodynamics. Combining this observation with the high entropy of facies across the depth and hydrodynamic gradients recorded in the focus areas (Fig. 3), the premise of ‘low-energy’ and ‘high-energy’ facies also becomes somewhat arbitrary. This observation suggests that the kind of depositional models typically used to describe, synthesize and predict carbonate facies

heterogeneity in shallow-water systems might be over simplistic.

The lack of relation between the lateral continuity of facies belts, depth and wave height can possibly be explained by the fact that the majority of the two mapped depositional systems: (i) have not built to sea-level, and particularly large areas of under-filled accommodation exist (subtidal deposits dominate over peritidal); and (ii) lie above storm weather wave base. Because the diversity of low-energy and zero-depth facies is low, lateral continuity of lithofacies is typically highest when relative water depth increases during flooding of the platform top, establishing low-energy subtidal conditions across the whole platform and when the accommodation has filled with tidal flat facies (e.g. Verwer *et al.*, 2009). Although tidal flat sediments are typically incised by channels, they do not fragment into a complex facies mosaic (Rankey, 2002; Maloof & Grotzinger, 2012). Given the large extent and zero water depth of the tidal flat, a relation between depth and facies type can be anticipated on platforms with filled, or nearly filled, accommodation, although the range in water depths will be narrow. From the stratigraphic perspective, however, even if the top of an upward shallowing cycle is homogeneous, this study suggests that the subtidal strata within the cycle will not be. Therefore, even during catch-up followed by keep-up accumulation, for example in a low accommodation greenhouse platform (e.g. Strasser, 1988; Jenkyns & Wilson, 1999; Spengler & Read, 2010), there is little reason to assume that the historic situation would be radically different from this modern example.

Facies extents are described by scaling laws

For each facies type in the two focus areas, the existence of a power law reports that the frequency of occurrence of a body is directly related to its areal extent by an invariant scale factor (the slope of the distributions in Figs 7 and 8). Power-law behaviour facilitates prediction across scale because an exponential decrease in probability of encounter for each facies body is coupled to an exponential decrease in unit area. For instance, knowledge of the number of wackestone bodies in Ras Al-Qasabah with areas $>1 \text{ km}^2$ would allow the number of bodies in that seascape with an area of 100 m^2 to be estimated, and so on. Such ‘scale invariance’ is helpful for sedimentologists

and stratigraphers working with ancient strata in outcrop, core, or even seismic because the occurrence of small facies bodies, which are typically challenging to detect, can be indirectly inferred from the frequency of large ones (Purkis *et al.*, 2007; Purkis *et al.*, 2012a; Harris *et al.*, 2011).

Wave and tide influence on the arrangement of photic zone carbonates

The term ‘fair weather wave base’ refers to the depth beneath the waves at which sufficient water motion exists to agitate the sea floor by everyday wave action. ‘Storm wave base’ refers to the depths beneath storm-driven waves and can be much deeper. The position of the fair weather and storm wave bases might be relevant to the heterogeneity of a subtidal facies mosaic because, conceptually, the process of wave sweeping and redistribution of soft sea floor sediment can promote lateral complexity (e.g. Seguret *et al.*, 2001; Flemming, 2005; Eberli, 2013). However, as recognized by Immenhauser (2009) and Peters & Loss (2012), and as evident in the wave height models, the spectrum of wave patterns is intriguingly complex across the varied depositional topography that typically develops atop carbonate platforms and, therefore, there is no such thing as an average fair weather or storm weather wave base that can be applied platform-wide, although storm events probably remain relevant (e.g. Cordier *et al.*, 2012; Madden *et al.*, 2013). According to the calculations of Clifton & Dingler (1984), the 3 m H_{m0} calculated for the exposed ocean-facing reef rims of Ras Al-Qasabah and Al Wajh is sufficient to impart orbital velocities of 1.0 m sec^{-1} down to water depths of *ca* 15 m. Behind the reef rim, where H_{m0} is the range of 1 m, this level of water movement remains at depths of *ca* 5 m. It should be noted that H_{m0} describes the mean of the 33% highest waves and so wave sweeping during rare storm events is likely to extend considerably deeper. On the basis of these values, *ca* 90% of the mapped sea floor of Ras Al-Qasabah and *ca* 80% of Al Wajh are within the range of regular wave agitation. These calculations can be considered conservative, because both focus areas display deep lagoons which are seawardly rimmed by an aggraded reef barrier. In Ras Al-Qasabah and Al Wajh, the rim is punctuated by a small number of channels through which water is exchanged on the changing tide. This restriction to flow can be anticipated to create

complex bottom currents that further serve to transport sediment, in turn promoting complex lateral facies patterns, as partly revealed in the models of Burgess & Wright (2003) and Hill *et al.* (2009). Following the nomenclature of Lagoe (1988), the 40 m depth limit of the present study corresponds to the lower boundary of the inner neritic zone. Deeper seabeds, such as those in the outer neritic zone extending from 40 m to 150 m water depth, experience little if any influence from surface waves and currents and therefore can be predicted to host less complex facies mosaics than witnessed in the inner neritic zone. As for the case of tidal flats, outer neritic seabeds may well display relations between the size of facies bodies and water depth and, as recognized by Rankey (2004), when depth variations of hundreds of metres are considered, that: “at a scale of shelf-to-basin transects, facies and habitats clearly are related to water depth”.

While the long-term winnowing effects of tides can be a systematic and large force in steering facies organization (Immenhauser, 2009), spring and neap tidal ranges are only 0.5 m and 0.05 m, respectively, in the northern Red Sea (Sheppard *et al.*, 1992; Sultan *et al.*, 1995). In such a microtidal regime, sediment redistribution by swell is likely to dominate that occurring due to tides (Cordier *et al.*, 2012), and strong tidal currents are unlikely to develop beyond those restricted to the narrow reef passes that connect the lagoons of both Ras Al-Qasabah and Al Wajh to the open ocean (as captured in the wave height model for Al Wajh, Fig. 3B) and these are of limited scale as compared to the extent of the overall depositional system.

The strongest relation between seabed character and hydrodynamic exposure exists for reef builders who, as recognized by Darwin (1842), despite the continuous damage from breaking waves, grow best on their ocean-facing side and grow rapidly even though they are bathed in low-nutrient waters of the subtropics. Quantitative field observations and laboratory experiments on reef-building corals offer two important insights: (i) corals grow faster in strong currents (Sebens *et al.*, 1998; Schutter *et al.*, 2010) and are more resistant against bleaching and other crises in high-current settings (Nakamura & van Woessik, 2001); and (ii) growth is impeded by sediment that settles on the coral surface (Rogers, 1990) with fine organic-rich sediment appearing to be more damaging than sand (Weber *et al.*, 2006). Both

factors clearly favour the wave-exposed edge position over the protected centre position in reefs on carbonate platforms (Schlager & Purkis, 2013) and explain why the prevalence of boundstone should be anticipated to increase with increasing wave energy, as is the case for the two focus areas (Figs 5 and 6). Although lacking the direct biotic link to water movement, the lateral variability of sediment types that arise from differences in rates of grain production and redistribution across hydrodynamic gradients are well-understood (e.g. Piller & Pervesler, 1989; Rankey & Reeder, 2011; Gischler *et al.*, 2013). For this reason, it is to be expected that wave height offers some control on the lateral placement of wackestone, grainstone and rudstone, as mapped in the two focus areas, and the statistical association with this parameter is logical.

Comparison of the facies maps with bathymetric models reveal that grain and mud-dominated textures appear with approximately equal frequency between water depths of 5 m and 25 m, a range that straddles the zone of maximum carbonate productivity (<10 m; Schlager, 1981). While the remote sensing data only offer a planimetric view at a snapshot in time, it is reasonable to assume that a degree of facies heterogeneity similar to the lateral will be preserved in the vertical stack of subtidal carbonate beds that accumulate through time. Because this analyses suggests that the intrinsic process of wave sweeping and redistribution of sediment may exercise as strong a control on facies character as water depth, the results support Wilkinson *et al.* (1996) and the forward model-based conclusions of Burgess & Wright (2003) and Burgess (2006), and caution the use of variations in depositional texture of lithofacies from the physical rock record to hindcast high-frequency sea-level cycles.

Is the allogenic-autogenic distinction useful?

Just as for the blind belief that subtidal facies in carbonate cycles can be precisely tied to water depths, attempting to pin sediment accumulation in the geological record to either allogenic or autogenic control is probably an oversimplification. Both processes yield interrelated and interacting parameters. For instance, allogenic changes in the position of sea-level not only alter water depth but also effect a host of other physical factors relevant to sedimentation in the photic zone, of which some would arguably be

classified as autogenic, including current patterns, water quality, the position on the platform where waves break, gradients of hydrodynamic exposure, temperature, chemistry, nutrients and so on. Changes to these physical factors promote different ecological niches that, in turn, serve to alter the biological workers of the carbonate factory and the types and quantities of grains that they produce – an autogenic effect. Therefore, as interpreted by Strasser (1988) in Cretaceous outcrops and modelled by Burgess & Wright (2003), at any point in time, a platform can consist of a spatially highly complex mosaic of carbonate factories, each controlled by local autogenic processes that can be overprinted by allogenic changes in sea-level affecting the whole platform. That is, allogenic controls evoke a host of autogenic processes and, therefore, seeking to disentangle their influences is unlikely to yield a satisfactory understanding of platform-top stratigraphy, begging the question as to how useful these designations are. While the present study shows a high degree of facies substitutability with water depth, it should not be taken to evidence a lack of allogenic control on the system. Indeed, in the context of the models proposed by Wright & Burgess (2005), such facies heterogeneity should be expected in both the modern and fossil record alike.

CONCLUSIONS

The satellite facies and bathymetry maps highlight the lateral heterogeneity of sediment accumulation across the two focus areas and their varied depositional topography. Statistical interrogation reveals the competing extra-platform and intra-platform controls that combine to deliver this complex lateral facies patterning. On the basis of Akaike information criterion (AIC) analysis, this study does not show facies type to be decoupled from water depth and hydrodynamics, but it does suggest that facies type cannot be confidently inferred from either parameter in isolation. By considering curves of cumulative probability for the occurrence of each facies across binned water depths, the degree to which palaeo-water depths might be predicted from ancient strata is examined. If the four facies mapped in this study were stacked in outcrop in such a way as to be interpreted as coarsening upwards, by standard interpretation, the sequence would be deemed to have been deposited under a regime of pro-

gressively shallowing water depth. Lacking a cap of peritidal facies, this bedding pattern contains the building blocks of a subtidal carbonate cycle. However, contrasting this hypothetical stacking pattern with the statistical distribution of facies by water depth yields little evidence that the stack shallows upwards. While there are no precise parallels between this modern study and the rock record, the comparison between the two is interesting and this hypothetical example highlights the pitfalls of assuming that a sea-level history can be inferred from ancient strata because subtidal carbonate facies neatly partition by water depth of deposition. The mapped facies occur in broad and overlapping depth ranges and, under such auspices, difficulties can be anticipated in the unequivocal identification of high-frequency subtidal carbonate cycles. The lateral extents of the considered facies are unrelated to water depth and wave height, but the plan-view size of facies bodies is related to their frequency of occurrence by a power law. The implication of the latter property being that small facies bodies, which are typically challenging to detect in fossil settings, can be indirectly inferred from the frequency of large ones. Such results broaden the perspective of the types of information that can be reliably extracted from the rock record of carbonates deposited in the shallow photic zone.

ACKNOWLEDGEMENTS

This paper was stimulated by a chance email from Bruce Wilkinson and has benefited from productive discussion through the years with Mitch Harris, Wolfgang Schlager and Andy Bruckner. Insightful reviews of the work were returned by Klaas Verwer, Peter Burgess, Associate Editor John Reijmer and Editor Tracy Frank, for which we are grateful. Financial support was provided by the National Coral Reef Institute (NCRI) and the Khaled bin Sultan Living Oceans Foundation (KBSLOF). Invaluable logistical field support was provided by the crew of the *M/Y Golden Shadow*, through the generosity of HRH Prince Khaled bin Sultan. Additional in-country support was provided by the Saudi Wildlife Commission (SWC) and PERSGA. Thanks are extended to Brett Thomasie and DigitalGlobe Inc. for assistance with satellite image acquisition. This is NCRI publication 155.

REFERENCES

- Aigner, T.A.** (1985) *Storm Depositional Systems: Dynamic Stratigraphy in Modern and Ancient Shallow-Marine Sequences*. Springer-Verlag, Dordrecht, 174 pp.
- Akaike, H.** (1973) Information theory and an extension of the maximum likelihood principle. In: *Breakthroughs in Statistics, Vol. 1, Foundations and Basic Theory* (Eds S. Kotz and N.L. Johnson), pp. 610–624. Springer-Verlag, New York, USA.
- Allen, J.R.L.** (1979) A model for the interpretation of wave ripple-marks using their wavelength, textural composition, and shape. *J. Geol. Soc. London*, **136**, 673–682.
- Andréfouët, S., Gabioch, G., Flamand, B. and Pelletier, B.** (2009) A reappraisal of the diversity of geomorphological and genetic processes of New Caledonian coral reefs: a synthesis from optical remote sensing, coring and acoustic multibeam observations. *Coral Reefs*, **28**, 691–707.
- Arz, H.W., Lamy, F., Patzold, J., Muller, P.J. and Prins, M.** (2003) Mediterranean moisture source for an early-Holocene humid period in the northern Red Sea. *Science*, **300**, 118–121.
- Augustin, N.H., Muggleston, M.A. and Buckland, S.T.** (1996) An autologistic model for the spatial distribution of wildlife. *J. Appl. Ecol.*, **33**, 339–347.
- Bosence, D.** (2008) Randomness or order in the occurrence and preservation of shallow-marine carbonate facies? Holocene, South Florida. *Palaeogeogr. Palaeoclimatol. Palaeoecol.*, **270**, 339–348.
- Burgess, P.M.** (2001) Modeling carbonate sequence development without relative sea-level oscillations. *Geology*, **29**, 1127–1130.
- Burgess, P.M.** (2006) The signal and the noise: forward modelling of autocyclic and allocyclic processes influencing peritidal stacking patterns. *J. Sed. Res.*, **76**, 962–977.
- Burgess, P.M. and Pollitt, D.A.** (2012) The origins of shallow-water carbonate lithofacies thickness distributions: one-dimensional forward modelling of relative sea-level and production rate control. *Sedimentology*, **59**, 57–80.
- Burgess, P.M. and Wright, V.P.** (2003) Numerical forward modelling of carbonate platform dynamics: an evaluation of complexity and completeness in carbonate strata. *J. Sed. Res.*, **73**, 637–652.
- Burgess, P.M., Wright, V.P. and Emery, D.** (2001) Numerical forward modelling of peritidal carbonate parasequence development: implications for outcrop interpretation. *Basin Res.*, **13**, 1–16.
- Burnham, K.P. and Anderson, D.R.** (2002) *Model Selection and Multimodel Inference: A Practical Information-Theoretic Approach*. Springer-Verlag, New York, USA.
- Calvet, F. and Tucker, M.E.** (1988) Outer ramp cycles in the Upper Muschelkalk of the Catalan basin, northeast Spain. *Sed. Geol.*, **57**, 185–198.
- Chollett, I. and Mumby, P.J.** (2012) Predicting the distribution of *Montastraea* reefs using wave exposure. *Coral Reefs*, **31**, 493–503.
- Clauset, A., Shalizi, C.R. and Newman, M.E.J.** (2009) Power-law distributions in empirical data. *Soc. Ind. Appl. Math. Rev.*, **51**, 661–703.
- Clifton, H.E. and Dingler, J.R.** (1984) Wave-formed structures and paleoenvironmental reconstruction. *Mar. Geol.*, **60**, 165–198.
- Cordier, E., Poizot, E. and Méar, Y.** (2012) Swell impact on reef sedimentary processes: a case study of La Reunion fringing reef. *Sedimentology*, **59**, 2004–2023.

- Darwin, C.R.** (1842) *The Structure and Distribution of Coral Reefs*, reprint edn. The University of Arizona Press, Tucson.
- Davies, C.P.** (2006) Holocene paleoclimates of southern Arabia from lacustrine deposits of the Dhamar highlands, Yemen. *Quatern. Res.*, **66**, 454–464.
- Dexter, T.A., Kowaleski, M. and Read, J.F.** (2009) Distinguishing Milankovitch-driven processes in the rock record from stochasticity using computer-simulated stratigraphy. *J. Geol.*, **117**, 349–361.
- Diedrich, N.W. and Wilkinson, B.H.** (1999) Depositional cyclicity in the Lower Devonian Helderberg Group of New York State. *J. Geol.*, **107**, 643–658.
- Dunham, R.J.** (1962) Classification of carbonate rocks according to depositional texture. In: *Classification of Carbonate Rocks* (Ed. W.E. Ham), *AAPG Mem.*, **1**, 108–121.
- Eberli, G.P.** (2013) The uncertainties involved in extracting amplitude and frequency of orbitally driven sea-level fluctuations from shallow-water carbonate cycles. *Sedimentology*, **60**, 64–84.
- Ekeboom, J., Laihonon, P. and Suominen, T.** (2003) A GIS-based step-wise procedure for assessing physical exposure in fragmented archipelagos. *Estuar. Coast. Shelf Sci.*, **57**, 887–898.
- Embry, A.F. and Klovan, J.E.** (1971) A late Devonian reef tract on northeastern Banks Island, N.W.T. *Bull. Can. Petrol. Geol.*, **19**, 730–781.
- Eriksson, K.A. and Simpson, E.L.** (1990) Recognition of high-frequency sea-level fluctuations in Proterozoic siliciclastic tidal deposits, Mount Isa, Australia. *Geology*, **18**, 474–477.
- Fischer, A.G.** (1964) The Lofer cyclothems of the Alpine Triassic. In: *Symposium on Cyclic Sedimentation* (Ed. D.F. Meriam), *Bull. Kansas State Geol. Surv.*, **169**, 107–149.
- Flemming, B.W.** (2005) The concept of wave base: fact and fiction. In: *Abstracts Sediment* (Eds H. Haas, K. Ramseyer and F. Schlunegger), pp. 57. Schriftenreihe der Deutschen Gesellschaft für Geowissenschaften, Heft, Gwatt, Lake Thun, Switzerland.
- Fournier, F., Borgomano, J. and Montaggioni, L.F.** (2005) Development patterns and controlling factors of Tertiary carbonate buildups: insights from high-resolution 3D seismic and well data in the Malampaya gas field (Offshore Palawan, Philippines). *Sed. Geol.*, **175**, 189–215.
- Ginsburg, R.N.** (1956) Environmental relationships of grain size and constituent particles in some south Florida carbonate sediments. *AAPG Bull.*, **40**, 2384–2427.
- Ginsburg, R.N.** (1971) Landward movement of carbonate mud: new model for regressive cycles in carbonates. *AAPG Conv. Abstr.*, **55**, 340.
- Ginsburg, R.N.** (1975) *Tidal Deposits*. Springer-Verlag, Dordrecht, 428 pp.
- Gischler, E., Dietrich, S., Harris, D., Webster, J.M. and Ginsburg, R.N.** (2013) A comparative study of modern carbonate mud in reefs and carbonate platforms: mostly biogenic, some precipitated. *Sed. Geol.*, **292**, 36–55.
- Goldhammer, R.K., Dunn, P.A. and Hardie, L.A.** (1987) High frequency glacio-eustatic sea level oscillations with Milankovitch characteristics recorded in Middle Triassic platform carbonates in northern Italy. *Am. J. Sci.*, **287**, 853–892.
- Goodwin, P.W. and Anderson, E.J.** (1985) Punctuated aggradational cycles: a general hypothesis of episodic stratigraphic accumulation. *J. Geol.*, **93**, 515–533.
- Graus, R.R. and Macintyre, I.G.** (1989) The zonation patterns of Caribbean coral reefs as controlled by wave and light energy input, bathymetric setting and reef morphology: computer simulation experiments. *Coral Reefs*, **8**, 9–18.
- Grötsch, J. and Mercadier, C.** (1999) Integrated 3-D reservoir modeling based on 3-D seismic: the Tertiary Malampaya and Camago buildups, offshore Palawan, Philippines. *AAPG Bull.*, **83**, 1703–1728.
- Grotzinger, J.P.** (1986) Cyclicity and paleoenvironmental dynamics, Rocknest platform, northwest Canada. *Geol. Soc. Am. Bull.*, **97**, 1208–1231.
- Handford, C.R. and Loucks, R.G.** (1993) Carbonate depositional sequences and systems tracts – responses of carbonate platforms to relative sea-level changes. In: *Carbonate Sequence Stratigraphy: Recent Developments and Applications* (Eds B. Loucks and R.J. Sarg), *AAPG Bull.*, **57**, 3–41.
- Harris, P.M., Purkis, S.J. and Ellis, J.** (2011) Analyzing spatial patterns in modern carbonate sand bodies from Great Bahama Bank. *J. Sed. Res.*, **81**, 185–206.
- Hill, J., Tetzlaff, D.M., Curtis, A. and Wood, R.** (2009) Modeling shallow marine carbonate depositional systems. *Comput. Geosci.*, **35**, 1862–1874.
- Hill, J., Wood, R., Curtis, A. and Tetzlaff, D.M.** (2012) Preserving of forcing signals in shallow water carbonate sediments. *Sed. Geol.*, **275–276**, 79–92.
- Hinnov, L.A. and Goldhammer, R.K.** (1991) Spectral analysis of the Middle Triassic Latemar limestone. *J. Sed. Petrol.*, **61**, 1173–1183.
- Immenhauser, A.** (2009) Estimating palaeo-water depth from the physical rock record. *Earth-Sci. Rev.*, **96**, 107–139.
- James, N.P.** (1984) Shallowing-upward sequences in carbonates. In: *Facies Models* (Ed. R.G. Walker), *Geosci. Can. Repr. Ser.*, **1**, 213–228.
- Jenkyns, H. and Wilson, P.A.** (1999) Stratigraphy, paleogeography, and evolution of Cretaceous Pacific guyots: relicts from a greenhouse earth. *Am. J. Sci.*, **299**, 341–392.
- Kenter, J.A.M., Harris, P.M., Weber, L.J., Collins, J.F., Kuanysheva, G. and Fischer, D.J.** (2006) Late Visean to Bashkirian platform cyclicity in the Central Tengiz buildup, Pricaspian Basin, Kazakhstan: depositional evolution and reservoir development. In: *Giant Hydrocarbon Reservoirs of the World: From Rocks to Reservoir Characterization and Modeling* (Eds P.M. Harris and L.J. Weber), *AAPG Mem.*, **88**, 7–54.
- Lagoe, M.B.** (1988) An evaluation of Paleogene paleobathymetric models; benthic foraminiferal distributions in the Metrella Member of the Tejon Formation, Central California. *Palaio*, **3**, 523–536.
- Laporte, L.** (1967) Carbonate deposition near mean sea-level and resultant facies mosaic: Manilus Formation (Lower Devonian) of New York State. *AAPG Bull.*, **51**, 73–101.
- Legendre, P.** (1993) Spatial autocorrelation: trouble or new paradigm? *Ecology*, **74**, 1659–1673.
- Liebau, A.** (1984) Grundlagen der Ökobathymetrie. In: *Paläobathymetrie. Palaeontol. Kursb.* (Ed. H. Luterbacher), pp. 149–184.
- Logan, B.W., Davies, G.R., Read, J.F. and Cebulski, D.** (1970) Carbonate sedimentation and environments, Shark Bay, Western Australia. *AAPG Mem.*, **13**, 223 pp.
- Madden, R.H.C., Wilson, M.E.J. and O'Shea, M.** (2013) Modern fringing reef carbonates from equatorial SE Asia:

- an integrated environmental, sediment and satellite characterization study. *Mar. Geol.*, **344**, 163–185.
- Malooof, A.C. and Grotzinger, J.P.** (2012) The Holocene shallowing-upward parasequences of north-west Andros Island, Bahamas. *Sedimentology*, **59**, 1375–1407.
- Markello, J.R. and Read, J.F.** (1982) Upper Cambrian intrashelf basin, Nolichucky Formation, southwest Virginia Appalachians. *AAPG Bull.*, **66**, 860–878.
- Meyers, S.R.** (2008) Resolving Milankovitchian controversies: the Triassic Latemar Limestone and the Eocene Green River Formation. *Geology*, **36**, 319–322.
- Nakamura, T. and van Woesik, R.** (2001) Water-flow rates and passive diffusion partially explain differential survival of corals during the 1998 bleaching event. *Mar. Ecol. Prog. Ser.*, **212**, 301–304.
- Osleger, D.** (1991) Subtidal carbonate cycles: implications for allocyclic vs. autocyclic controls. *Geology*, **19**, 917–920.
- Peterhänsel, A. and Egenhoff, S.O.** (2008) Lateral variabilities of cycle stacking patterns in the Latemar, Triassic, Italian Dolomites. In: *Controls on Carbonate Platform and Reef Development* (Eds J. Lukasik and J.A.T. Simo), *SEPM Spec. Publ.*, **78**, 217–229.
- Peters, S.E. and Loss, D.P.** (2012) Storm and fair-weather wave base: a relevant distinction? *Geology*, **40**, 511–514.
- Piller, W.E. and Pervesler, P.** (1989) The Northern Bay of Safaga (Red Sea, Egypt): an actiopalaontological approach, I. topography and bottom facies. *Beitr. Paläontol. Österr.*, **15**, 103–147.
- Pomar, L.** (2001) Types of carbonate platforms: a genetic approach. *Basin Res.*, **13**, 313–334.
- Pratt, B.R. and James, N.P.** (1986) The St. George Group (Lower Ordovician) of western Newfoundland: tidal flat island model for carbonate sedimentation in shallow epeiric seas. *Sedimentology*, **33**, 313–343.
- Purdy, E.G. and Gischler, E.** (2003) The Belize margin revisited: 1. Holocene marine facies. *Int. J. Earth Sci.*, **92**, 532–551.
- Purkis, S.J. and Riegl, B.** (2005) Spatial and temporal dynamics of Arabian Gulf coral assemblages quantified from remote-sensing and in situ monitoring data. *Mar. Ecol. Prog. Ser.*, **287**, 99–113.
- Purkis, S.J. and Vlaswinkel, B.** (2012) Visualizing lateral anisotropy in modern carbonates. *AAPG Bull.*, **96**, 1665–1685.
- Purkis, S.J., Riegl, B. and Andréfouët, S.** (2005) Remote sensing of geomorphology and facies pattern on a modern carbonate ramp (Arabian Gulf, Dubai, U.A.E.). *J. Sed. Res.*, **75**, 861–876.
- Purkis, S.J., Kohler, K.E., Riegl, B.M. and Rohmann, S.E.** (2007) The statistics of natural shapes in modern coral reef landscapes. *J. Geol.*, **115**, 493–508.
- Purkis, S.J., Rowlands, G.P., Riegl, B.M. and Renaud, P.G.** (2010) The paradox of tropical karst morphology in the coral reefs of the arid Middle East. *Geology*, **38**, 227–230.
- Purkis, S.J., Harris, P.M. and Ellis, J.** (2012a) Patterns of sedimentation in the contemporary Red Sea as an analog for ancient carbonates in rift settings. *J. Sed. Res.*, **82**, 859–870.
- Purkis, S.J., Vlaswinkel, B. and Gracias, N.** (2012b) Vertical-to-lateral transitions among Cretaceous carbonate facies – a means to 3-D framework construction via Markov analysis. *J. Sed. Res.*, **82**, 232–243.
- R Development Core Team** (2008). *R: A Language and Environment for Statistical Computing*. R Foundation for Statistical Computing, Vienna, Austria. ISBN 3-900051-07-0. Available at: <http://www.R-project.org>.
- Rankey, E.C.** (2002) Spatial patterns of sediment accumulation on a Holocene carbonate tidal flat, northwest Andros island, Bahamas. *J. Sed. Res.*, **72**, 591–601.
- Rankey, E.C.** (2004) On the interpretation of shallow shelf carbonate facies and habitats: how much does water depth matter? *J. Sed. Res.*, **74**, 2–6.
- Rankey, E.C. and Reeder, S.L.** (2011) Holocene oolitic marine sand complexes of the Bahamas. *J. Sed. Res.*, **81**, 97–117.
- Rankey, E.C., Guidry, S.A., Reeder, S.L. and Guarin, H.** (2009) Geomorphic and sedimentologic heterogeneity along a Holocene shelf margin: Caicos Platform. *J. Sed. Res.*, **79**, 440–456.
- Reijmer, J.J.G., Swart, P.K., Bauch, T., Otto, R., Reuning, L., Roth, S. and Zechel, S.** (2009) A re-evaluation of facies on Great Bahama Bank I: new facies maps of western Great Bahama Bank. *Int. Assoc. Sedimentol. Spec. Publ.*, **41**, 29–46.
- Riegl, B. and Piller, W.E.** (1999) Coral frameworks revisited – reefs and coral carpets in the northern Red Sea. *Coral Reefs*, **18**, 241–253.
- Rogers, C.S.** (1990) Responses of coral reefs and reef organisms to sedimentation. *Mar. Ecol. Prog. Ser.*, **62**, 185–202.
- Rohweder, J., Rogala, J.T., Johnson, B.L., Anderson, D., Clark, S., Chamberlin, F. and Runyon, K.** (2008) *Application of Wind Fetch and Wave Models for Habitat Rehabilitation and Enhancement Projects*. U.S. Geological Survey Open-File Report 2008–1200, 43 pp.
- Rowlands, G., Purkis, S.J., Riegl, B., Metsamaa, L., Bruckner, A. and Renaud, P.** (2012) Satellite imaging coral reef resilience at regional scale. A case-study from Saudi Arabia. *Mar. Pollut. Bull.*, **64**, 1222–1237.
- Rowlands, G., Purkis, S.J. and Bruckner, A.** (2014) Diversity in the geomorphology of shallow-water carbonate depositional systems in the Saudi Arabian Red Sea. *Geomorphology*, **86**, 117–134.
- Satterley, A.K.** (1996) The interpretation of cyclic successions of the Middle and Upper Triassic of the Northern and Southern Alps. *Earth Sci. Rev.*, **40**, 181–207.
- Schlager, W.** (1981) The paradox of drowned reefs and carbonate platforms. *Geol. Soc. Am. Bull.*, **92**, 197–211.
- Schlager, W.** (2003) Benthic carbonate factories of the Phanerozoic. *Int. J. Earth Sci.*, **92**, 445–464.
- Schlager, W. and Purkis, S.J.** (2013) Bucket structure in carbonate accumulations of the Maldives, Chagos and Laccadive archipelagos. *Int. J. Earth Sci.*, **102**, 2225–2238.
- Schutter, M., Croker, J., Paijmans, A., Janse, M., Osinga, R., Verreth, A.J. and Wijffels, R.H.** (2010) The effect of different flow regimes on the growth and metabolic rates of the scleractinian coral *Galaxea fascicularis*. *Coral Reefs*, **29**, 737–748.
- Schwarzacher, W.** (2000) Repetitions and cycles in stratigraphy. *Earth Sci. Rev.*, **50**, 51–75.
- Sebens, K.P., Grace, S.O., Helmuth, B., Maney, E.J. and Miles, J.S.** (1998) Water flow and prey capture by three scleractinian corals, *Madracis mirabilis*, *Montastera cavernosa* and *Porites porites*, in a field enclosure. *Mar. Biol.*, **131**, 347–360.
- Seguret, M., Moussine-Pouchkine, A., Raja Gabaglia, G. and Bouchette, F.** (2001) Storm deposits and storm-generated coarse carbonate breccias on a pelagic outer shelf (South-East Basin, France). *Sedimentology*, **48**, 231–254.

- Shannon, C.E.** (1948) A mathematical theory of communication. *Bell Syst. Tech. J.*, **27**, 379–423.
- Sheppard, C.R.C.** (1982) Coral populations on reef slopes and their major controls. *Mar. Ecol. Prog. Ser.*, **7**, 83–115.
- Sheppard, C., Price, A. and Roberts, C.** (1992) *Marine Ecology of the Arabian Region. Patterns and Processes in Extreme Tropical Environments*. Academic Press, London, 359 pp.
- Shinn, E.A., Lloyd, R.M. and Ginsburg, R.N.** (1969) Anatomy of a modern carbonate tidal flat, Andros Island, Bahamas. *J. Sed. Petrol.*, **39**, 1202–1228.
- Spengler, A.E. and Read, J.F.** (2010) Sequence development on a sediment-starved, low accommodation epeiric carbonate ramp: silurian Wabash Platform, USA mid-continent during icehouse to greenhouse transition. *Sed. Geol.*, **224**, 84–115.
- Strasser, A.** (1988) Shallowing-upward sequences in Purbeckian peritidal carbonates (lowermost Cretaceous, Swiss and French Jura Mountains). *Sedimentology*, **35**, 369–383.
- Strasser, A.** (1991) Lagoonal-peritidal sequences in carbonate environments: autocyclic and allocyclic processes. In: *Cycles and Events in Stratigraphy* (Eds G. Einsele, W. Ricken and A. Seilacher), pp. 709–721. Springer, Berlin.
- Strasser, A., Pittet, B., Hillgärtner, H. and Pasquier, J.-B.** (1999) Depositional sequences in shallow-dominated sedimentary systems: concepts for a high-resolution analysis. *Sed. Geol.*, **128**, 201–221.
- Stumpf, R.P., Holderied, K. and Sinclair, M.** (2003) Determination of water depth with high-resolution satellite imagery over variable bottom types. *Limnol. Oceanogr.*, **48**, 547–556.
- Sultan, S.A.R., Ahmad, F. and El-Hassan, A.** (1995) Seasonal variation of the sea level in the central part of the Red Sea. *Estuar. Coast. Shelf Sci.*, **40**, 1–8.
- Sundquist, B.** (1982) Palaeobathymetric interpretation of wave ripple-marks in a Ludlovian grainstone of Gotland. *Geol. Fören. Stockh. Förh.*, **104**, 157–166.
- Tucker, M.E.** (1990) Geological background to carbonate sedimentation. In: *Carbonate Sedimentology* (Eds M.E. Tucker and V.P. Wright), pp. 28–69. Blackwell Scientific Publications, Oxford.
- Verwer, K., Della Porta, G., Merino-Tomé, O. and Kenter, J.A.M.** (2009) Controls and predictability of carbonate facies architecture in a Lower Jurassic three-dimensional barrier-shoal complex (Djebel Bou Dahar, High Atlas, Morocco). *Sedimentology*, **56**, 1801–1831.
- Wanless, H.R.** (1981) Fining-upward sedimentary sequences generated in seagrass beds. *J. Sed. Petrol.*, **51**, 445–454.
- Weber, L.J., Francis, B.P., Harris, P.M. and Clark, M.** (2003) Stratigraphy, facies, and reservoir characterization – Tengiz Field, Kazakhstan. In: *Permo-Carboniferous Carbonate Platforms and Reefs* (Eds W.M. Ahr, P.M. Harris, W.A. Morgan and I. Somerville), *AAPG Mem.*, **83**, 351–394.
- Weber, M., Lott, C. and Fabricius, K.E.** (2006) Sedimentation stress in a scleractinian coral exposed to terrestrial and marine sediments with contrasting physical, organic and geochemical properties. *J. Exp. Mar. Biol. Ecol.*, **336**, 18–32.
- Wehrmann, A., Hertweck, G., Brocke, R., Jansen, U., Königshof, P., Plodowski, G., Schindler, E., Wilde, V., Blicke, A. and Schultka, S.** (2005) Paleoenvironment of an Early Devonian land–sea transition: a case study from the southern margin of the Old Red Continent (Mosel Valley, Germany). *Palaios*, **20**, 101–120.
- Wilkinson, B.H. and Drummond, C.N.** (2004) Facies mosaics across the Persian Gulf and around Antigua – stochastic and deterministic products of shallow-water sediment accumulation. *J. Sed. Res.*, **74**, 513–526.
- Wilkinson, B.H., Diedrich, N.W. and Drummond, C.N.** (1996) Facies successions in peritidal carbonate sequences. *J. Sed. Res.*, **66**, 1065–1078.
- Wilkinson, B.H., Drummond, C.N., Diedrich, N.W. and Rothman, E.D.** (1999) Poisson processes of carbonate accumulation on Paleozoic and Holocene platforms. *J. Sed. Res.*, **69**, 338–350.
- Wright, V.P. and Burchette, T.P.** (1996) Shallow-water carbonate environments. In: *Sedimentary Environments: Processes, Facies and Stratigraphy* (Ed. H.G. Reading), pp. 325–394. Blackwell Science Ltd, Oxford.
- Wright, V.P. and Burgess, P.M.** (2005) The carbonate factory continuum, facies mosaics and microfacies: an appraisal of some of the key concepts underpinning carbonate sedimentology. *Facies*, **51**, 19–25.

Manuscript received 11 July 2013; revision accepted 23 January 2014